Lecture Notes in Mechanical Engineering

Vitalii Ivanov · Justyna Trojanowska · Ivan Pavlenko · Jozef Zajac · Dragan Peraković *Editors*

Advances in Design, Simulation and Manufacturing IV

Proceedings of the 4th International Conference on Design, Simulation, Manufacturing: The Innovation Exchange, DSMIE-2021, June 8–11, 2021, Lviv, Ukraine – Volume 1: Manufacturing and Materials Engineering

Springer

Lecture Notes in Mechanical Engineering

Lecture Notes in Mechanical Engineering (LNME) publishes the latest developments in Mechanical Engineering—quickly, informally and with high quality. Original research reported in proceedings and post-proceedings represents the core of LNME. Volumes published in LNME embrace all aspects, subfields and new challenges of mechanical engineering. Topics in the series include:

- Engineering Design
- Machinery and Machine Elements
- Mechanical Structures and Stress Analysis
- Automotive Engineering
- Engine Technology
- Aerospace Technology and Astronautics
- Nanotechnology and Microengineering
- Control, Robotics, Mechatronics
- MEMS
- Theoretical and Applied Mechanics
- Dynamical Systems, Control
- Fluid Mechanics
- Engineering Thermodynamics, Heat and Mass Transfer
- Manufacturing
- Precision Engineering, Instrumentation, Measurement
- Materials Engineering
- Tribology and Surface Technology

To submit a proposal or request further information, please contact the Springer Editor of your location:

China: Ms. Ella Zhang at ella.zhang@springer.com
India: Priya Vyas at priya.vyas@springer.com
Rest of Asia, Australia, New Zealand: Swati Meherishi at swati.meherishi@springer.com
All other countries: Dr. Leontina Di Cecco at Leontina.dicecco@springer.com

To submit a proposal for a monograph, please check our Springer Tracts in Mechanical Engineering at http://www.springer.com/series/11693 or contact Leontina.dicecco@springer.com

Indexed by SCOPUS. All books published in the series are submitted for consideration in Web of Science.

More information about this series at http://www.springer.com/series/11236

Vitalii Ivanov · Justyna Trojanowska ·
Ivan Pavlenko · Jozef Zajac ·
Dragan Peraković
Editors

Advances in Design, Simulation and Manufacturing IV

Proceedings of the 4th International Conference on Design, Simulation, Manufacturing: The Innovation Exchange, DSMIE-2021, June 8–11, 2021, Lviv, Ukraine – Volume 1: Manufacturing and Materials Engineering

Springer

Editors
Vitalii Ivanov
Sumy State University
Sumy, Ukraine

Ivan Pavlenko
Sumy State University
Sumy, Ukraine

Dragan Peraković
University of Zagreb
Zagreb, Croatia

Justyna Trojanowska
Poznan University of Technology
Poznan, Poland

Jozef Zajac
Technical University of Kosice
Presov, Slovakia

ISSN 2195-4356 ISSN 2195-4364 (electronic)
Lecture Notes in Mechanical Engineering
ISBN 978-3-030-77718-0 ISBN 978-3-030-77719-7 (eBook)
https://doi.org/10.1007/978-3-030-77719-7

This Springer imprint is published by the registered company Springer Nature Switzerland AG
The registered company address is: Gewerbestrasse 11, 6330 Cham, Switzerland

Preface

This volume of Lecture Notes in Mechanical Engineering contains selected papers presented at the 4th International Conference on Design, Simulation, Manufacturing: The Innovation Exchange (DSMIE-2021), held in Lviv, Ukraine, on June 8–11, 2021. The conference was organized by the Sumy State University, Lviv Polytechnic National University, and International Association for Technological Development and Innovations, in partnership with Technical University of Kosice (Slovak Republic), Kielce University of Technology (Poland), University of West Bohemia (Czech Republic), Poznan University of Technology (Poland), Association for Promoting Innovative Technologies—Innovative FET (Croatia), and Society for Robotics of Bosnia and Herzegovina (Bosnia and Herzegovina).

DSMIE-2021 is the international forum for fundamental and applied research and industrial applications in engineering. The conference focuses on a broad range of research challenges in the fields of manufacturing, materials, mechanical, and chemical engineering, addressing current and future trends in design approaches, simulation techniques, computer-aided systems, innovative production approaches, Industry 4.0 strategy implementation for engineering tasks solving, and engineering education. DSMIE-2021 brings together researchers from academic institutions, leading industrial companies, and government laboratories worldwide to promote and popularize the scientific fundamentals of manufacturing.

DSMIE-2021 received 175 contributions from 27 countries around the world. After a thorough peer-review process, the program committee accepted 100 papers written by authors from 20 countries. Thank you very much to the authors for their contribution. These papers are published in the present book, achieving an acceptance rate of about 57%. Extended versions of selected best papers will be published in scientific journals: Management and Production Engineering Review (Poland), Archives of Mechanical Technology and Materials (Poland), Journal of Engineering Sciences (Ukraine), Advances in Thermal Process and Energy Transformation (Slovak Republic), and Assembly Techniques and Technologies (Poland).

We would like to thank members of the program committee and invited external reviewers for their efforts and expertise in contributing to reviewing, without which it would be impossible to maintain the high standards of peer-reviewed papers. Program committee members and invited external reviewers devoted their time and energy to peer-reviewing manuscripts. Our reviewers come from all over the world and represent 18 countries and are affiliated with more than 70 institutions.

Thank you very much to keynote speakers: Vitalii Pasichnyk (Ukraine), Katarzyna Antosz (Poland), and Alper Uysal (Turkey) for sharing their knowledge and experience.

The book “Advances in Design, Simulation and Manufacturing IV” was organized into two volumes according to the main conference topics: Volume 1—Manufacturing and Materials Engineering and Volume 2—Mechanical and Chemical Engineering. Each volume is devoted to research in design, simulation, and manufacturing in the main conference areas.

The first volume consists of five parts. The first part includes recent developments in product design and manufacturing processes. Notably, it presents ways for ensuring the technological parameters of automobile engines, studying the contact pressure in parts, the development of approaches for recognition cutting parts of cutters during machining, and fractal analysis of metal structures. This part also includes the research of spindle units for multi-operational lathes, technological inheritability and damageability of materials, studies of wear characteristics for hardened steels using laser–ultrasonic surface treatment, and rational design modeling of an interference fit. Recent developments in designing implants via additive technologies, dynamic modeling of automatic clamping mechanisms, optimal designing of automobile pipe adapters, and grinding hard alloys using solid lubricants are also presented in this part. Finally, the first part includes studies in ensuring technological parameters of surface shaping, design calculation of electrohydraulic drives and technological equipment, optimizing the interelectrode gap during electrical discharge grinding, and designing thread joints for thin-walled shells.

The second part includes studies in the implementation of intelligent solutions within the Industry 4.0 strategy. Notably, ways to implement blockchain information management systems and agile project management for IMS and IT projects are analyzed. This part also consists of optimization work with a digital human model, the implementation of Industry 4.0 supported by service robots in production processes, intelligent numerical control of profile grinding, and carrier behavior strategy. Autonomous data-driven integration systems, 3D technology radar models to evaluate emerging technologies, and ensuring the reliability of transport systems are also included. Finally, the second part presents an intelligent scheduling system architecture for manufacturing systems and a new approach for providing internal logistics according to Industry 4.0 concept and corresponding requirements.

The third part is devoted to contributing to ICT in engineering education. Mainly, it presents studies aimed at developing a mobile application for test control, integrated quality assurance at HEI, and Android application for explaining form deviations based on 3D models. This part also includes recent developments in in-campus transfer technology and information and communication technologies for enhancing engineering creativity.

The fourth part is based on numerical simulation and experimental studies of milling, honing, burnishing, turning, abrasive finishing, hobbing, fine boring, gear shaping, and abrasive processing. Ways for modeling crack formation during thermomechanical processing of materials and the study of the impact of heat flows on the machine tool's wheelhead are also presented in this part. Finally, the fourth part includes numerical, experimental, and statistical results for surface layer operational characteristics and machining parts under dry, MQL, and nanofluid MQL conditions.

The fifth part aims at presenting recent developments in advanced materials and their applications. Remarkably, ways for strengthening centrifugal pumps' shafts by chemical–thermocycling treatment are proposed. The influence of synthesis modes on ceramic coatings' properties is analyzed. Optimal composite shelled sandwich structures with a honeycomb filler are designed. Ways for preparation and characterization of biocomposites, advanced manufacturing technologies for obtaining high-quality castings, the ion bombardment modeling of nano-periodic composite structures, and the rational choice of material for orthopedic purposes are proposed. Finally, the fifth part presents investigations in surface bandage

We appreciate the partnership with Springer, StrikePlagiarism, EasyChair, and our sponsors for their essential support during the preparation of DSMIE-2021.

Thank you very much for DSMIE Team. Their involvement and hard work were crucial to the success of the conference.

DSMIE's motto is *"Together we can do more for science, technology, engineering, and education"*.

June 2021

Vitalii Ivanov
Justyna Trojanowska
Ivan Pavlenko
Jozef Zajac
Dragan Perakovic

Organization

Steering Committee

General Chair

Vitalii Ivanov	Sumy State University, Ukraine

Co-chair

Ihor Hrytsai	Lviv Polytechnic National University, Ukraine

Members

Oleksandr Gusak	Sumy State University, Ukraine
Yaroslav Kusyi	Lviv Polytechnic National University, Ukraine
Oleksandr Liaposhchenko	Sumy State University, Ukraine
Ivan Pavlenko	Sumy State University, Ukraine
Vadym Stupnytskyy	Lviv Polytechnic National University, Ukraine

Program Committee

Gabriel Abba	University of Lorraine, France
Jean-Francois Antoine	University of Lorraine, France
Katarzyna Antosz	Rzeszow University of Technology, Poland
Jose Manoel Balthazar	Institute of Aeronautics and Space, Brazil
Kristina Berladir	Sumy State University, Ukraine
Jozef Bocko	Technical University of Kosice, Slovak Republic
Ricardo Branco	University of Coimbra, Portugal
Dagmar Caganova	Slovak University of Technology, Slovak Republic
Emilia Campean	Technical University of Cluj-Napoca, Romania
Robert Cep	VSB-Technical University of Ostrava, Czech Republic

Yelizaveta Chernysh	Sumy State University, Ukraine
Olivian Chiver	Technical University of Cluj-Napoca, Romania
Vasile George Cioata	Polytechnic University of Timisoara, Romania
Olaf Ciszak	Poznan University of Technology, Poland
Oguz Colak	Eskisehir Technical University, Turkey
Radu Cotetiu	Technical University of Cluj-Napoca, Romania
Nadezda Cubonova	University of Zilina, Slovak Republic
Ivan Cvitic	University of Zagreb, Croatia
Predrag Dasic	University Union “Nikola Tesla,” Serbia
Yuliia Denysenko	Sumy State University, Ukraine
Oleksandr Derevianchenko	Odessa National Polytechnic University, Ukraine
Sergey Dobrotvorskiy	National Technical University “Kharkiv Polytechnic Institute,” Ukraine
Mihai Dragomir	Technical University of Cluj-Napoca, Romania
Kostiantyn Dyadyura	Sumy State University, Ukraine
Milan Edl	University of West Bohemia, Czech Republic
Sulaymon Eshkabilov	North Dakota State University, USA
Mathieu Gautier	University Lyon, France
Renata Gnatowska	Czestochowa University of Technology, Poland
Mihaly Gorbe	John von Neumann University, Germany
Marta Grabowska	Poznan University of Technology, Poland
Domenico Guida	University of Salerno, Italy
Oleksandr Gusak	Sumy State University, Ukraine
Michal Hatala	Technical University of Kosice, Slovak Republic
Ihor Hurey	Lviv Polytechnic National University, Ukraine
Vitalii Ivanov	Sumy State University, Ukraine
Maryna Ivanova	National Technical University “Kharkiv Polytechnic Institute,” Ukraine
Lydmila Kalafatova	Donetsk National Technical University, Ukraine
Isak Karabegovic	University of Bihac, Bosnia, and Herzegovina
Gennadii Khavin	National Technical University “Kharkiv Polytechnic Institute,” Ukraine
Lucia Knapcikova	Technical University of Kosice, Slovak Republic
Kateryna Kostyk	National Technical University “Kharkiv Polytechnic Institute,” Ukraine
Jan Krmela	Alexander Dubcek University of Trencin, Slovak Republic
Ivan Kuric	University of Zilina, Slovak Republic
Yaroslav Kusyi	Lviv Polytechnic National University, Ukraine
Vladimir Lebedev	Odessa National Polytechnic University, Ukraine
Oleksandr Liaposhchenko	Sumy State University, Ukraine
Slawomir Luscinski	Kielce University of Technology, Poland
Jose Mendes Machado	University of Minho, Portugal
Angelos Markopoulos	National Technical University of Athens, Greece
Mykola Melnychuk	Lutsk National Technical University, Ukraine

Ronald L. Mersky	Widener University, USA
Viktor Molnar	University of Miskolc, Hungary
Ronald Iosif Moraru	University of Petrosani, Romania
Dmitriy Muzylyov	Kharkiv Petro Vasylenko National Technical University of Agriculture, Ukraine
Marek Ochowiak	Poznan University of Technology, Poland
Daniela Onofrejova	Technical University of Kosice, Slovak Republic
Oleh Onysko	Ivano-Frankivsk National Technical University of Oil and Gas, Ukraine
Vitalii Pasichnyk	National Technical University of Ukraine "Kyiv Polytechnic Institute named after I. Sikorskyi," Ukraine
Ivan Pavlenko	Sumy State University, Ukraine
Dragan Perakovic	University of Zagreb, Croatia
Marco Perisa	University of Zagreb, Croatia
Oleksandr Permiakov	National Technical University "Kharkiv Polytechnic Institute," Ukraine
Jan Pitel	Technical University of Kosice, Slovak Republic
Grigore Marian Pop	Technical University of Cluj-Napoca, Romania
Oleksandr Povstyanoy	Lutsk National Technical University, Ukraine
Erwin Rauch	Free University of Bolzano, Italy
Michal Rogalewicz	Poznan University of Technology, Poland
Andrii Rogovyi	Kharkiv National Automobile and Highway University, Ukraine
Yiming Rong	Southern University of Science and Technology, China
Alessandro Ruggiero	University of Salerno, Italy
Vira Shendryk	Sumy State University, Ukraine
Robert Sika	Poznan University of Technology, Poland
Lesya Shkitsa	Ivano-Frankivsk National Technical University of Oil and Gas, Ukraine
Vsevolod Sklabinskyi	Sumy State University, Ukraine
Volodymyr Sokolov	V. Dahl East Ukrainian National University, Ukraine
Marcin Sosnowski	Jan Dlugosz University of Czestochowa, Poland
Vadym Stupnytskyy	Lviv Polytechnic National University, Ukraine
Antoni Swic	Lublin University of Technology, Poland
Yuliia Tarasevych	AGH University of Science and Technology, Poland
Volodymyr Tonkonogyi	Odessa National Polytechnic University, Ukraine
Justyna Trojanowska	Poznan University of Technology, Poland
Michael Tseitlin	National Technical University "Kharkiv Polytechnic Institute," Ukraine
Nicolae Ungureanu	Technical University of Cluj-Napoca, Romania
Alper Uysal	Yildiz Technical University, Turkey
Leonilde Rocha Varela	University of Minho, Portugal

George-Christopher Vosniakos	National Technical University of Athens, Greece
Jerzy Winczek	Czestochowa University of Technology, Poland
Szymon Wojcechowski	Poznan University of Technology, Poland
Oleg Zabolotnyi	Lutsk National Technical University, Ukraine
Jozef Zajac	Technical University of Kosice, Slovak Republic
Volodymyr Zavialov	National University of Food Technologies, Ukraine
Przemyslaw Zawadzki	Poznan University of Technology, Poland
Jan Zdebor	University of West Bohemia, Czech Republic
Lianyu Zheng	Beihang University, China
Predrag Zivkovic	University of Nis, Serbia

Invited External Reviewers

Frantisek Botko	Technical University of Kosice, Slovak Republic
Vladimir Bulej	University of Zilina, Slovak Republic
Alina Crisan	University of Agricultural Sciences and Veterinary Medicine, Romania
Liviu Adrian Crisan	Technical University of Cluj-Napoca, Romania
Maryna Demianenko	Sumy State University, Ukraine
Jan Gorecki	Poznan University of Technology, Poland
Damian Grajewski	Poznan University of Technology, Poland
Jakub Hajkowski	Poznan University of Technology, Poland
Nadiia Kharchenko	Sumy State University, Ukraine
Serhii Khovanskyi	Sumy State University, Ukraine
Vladyslav Kondus	Sumy State University, Ukraine
Dmytro Konovalov	Admiral Makarov National University of Shipbuilding, Ukraine
Ivan Kozii	Sumy State University, Ukraine
Dmytro Kryvoruchko	Sumy State University, Ukraine
Agnieszka Kujawinska	Poznan University of Technology, Poland
Stanislaw Legutko	Poznan University of Technology, Poland
Dmytro Levchenko	Innovative Solutions LLC, Ukraine
Svitlana Lugova	JSC Nasosenergomash Sumy, Ukraine
Janosch Luttmer	University of Duisburg-Essen, Germany
Oleh Lychak	Karpenko Physico-Mechanical Institute of the National Academy of Sciences of Ukraine, Ukraine
Dariusz Mazurkiewicz	Lublin University of Technology, Poland
Jakub Michalski	Poznan University of Technology, Poland
Iurii Merzliakov	Sumy State University, Ukraine
Panagiotis Karmiris Obratanski	National Technical University of Athens, Greece
Emmanouil Papazoglou	National Technical University of Athens, Greece

Robin Pluhnau	University of Duisburg-Essen, Germany
Mykola Radchenko	Admiral Makarov National University of Shipbuilding, Ukraine
Michal Sajgalik	University of Zilina, Slovak Republic
Serhii Sharapov	Sumy State University, Ukraine
Dimitrios Skondras-Giousios	National Technical University of Athens, Greece
Maksym Skydanenko	Sumy State University, Ukraine
Viktoriia Vakal	Sumy State University, Ukraine
Radoslaw Wichniarek	Poznan University of Technology, Poland
Dmytro Zhyhylii	Sumy State University, Ukraine

DSMIE Team

Kristina Berladir	Sumy State University, Ukraine
Oleksandr Gusak	Sumy State University, Ukraine
Ihor Hrytsai	Lviv Polytechnic National University, Ukraine
Vitalii Ivanov	Sumy State University, Ukraine
Yaroslav Kusyi	Lviv Polytechnic National University, Ukraine
Oleksandr Liaposhchenko	Sumy State University, Ukraine
Ivan Pavlenko	Sumy State University, Ukraine
Andrii Slipchuk	Lviv Polytechnic National University, Ukraine
Vadym Stupnytskyy	Lviv Polytechnic National University, Ukraine

Contents

Advanced Materials

Product Design and Manufacturing Processes

Ensuring the Technological Parameters of Cast Block Crankcase of Automobile's Diesel Engine

Oleg Akimov[1], Kateryna Kostyk[1(✉)], Stepan Klymenko[2], Pavel Penzev[1], and Leonid Saltykov[1]

[1] National Technical University "Kharkiv Polytechnic Institute", 2, Kyrpychova Street, Kharkiv 61002, Ukraine
[2] Physico-Technological Institute of Metals and Alloys of the National Academy of Sciences of Ukraine, 34/1, Vernadskogo Blvd., Kyiv 03142, Ukraine

Abstract. The relevance of computer-integrated technologies for manufacturing parts is significant in the world . The purpose of this work is to analyze the quality of cast block crankcase using a universal technology of complex computer-integrated design of cast parts of internal combustion engines using engineering modeling of thermal and hydrodynamic parameters of casting . The results of computer-engineering modeling of thermal and hydrodynamic processes of block crankcase casting have shown that gas-shrinkage defects can be stress concentrators in the part's structural elements. Therefore, they can affect the strength characteristics during operation. The developed 3D model of block crankcase casting with a technological gating-feeding system allowed creating a finite-difference model of casting and tooling and performing engineering modeling of casting processes in the ICS NovaFlow. The analysis of physical features of the processes of filling and cooling the castings in the mold was performed for the cast block crankcase of 4DTNA1 automobile diesel, the locations and sizes of gas-shrinkable defects were determined according to the Niyama criterion. The research results allowed us to form boundary and initial conditions for modeling the stress-strain state of the block crankcase in the places of gas-shrink porosity formation. Further development of the above studies will be carried out for castings of new types, configurations, other casting technologies, newly synthesized alloys.

Keywords: Solidworks · Novaflow · Block crankcase · Engines · 3D model · Casting defects

1 Introduction

Modern computer-aided design of cast engine parts is a powerful tool for developing new parts and upgrading existing ones. Current systems for computer-engineering modeling of production processes and analysis of the thermal and stress-strain state of cast parts of internal combustion engines are the most effective in design and technological design.

Processes computer-aided design, technological preparation, and production of cast engine parts are an integral part of a systematic approach inherent in the CALS-technologies, i.e., a set of the corresponding time sequence of state changes of the part.

V. Ivanov et al. (Eds.): DSMIE 2021, LNME, pp. 3–11, 2021.
https://doi.org/10.1007/978-3-030-77719-7_1

In current conditions, the main requirements for manufactured products are high quality, low cost, and minimum development time for new products, which can be achieved using computer modeling [1] and parameter identification [2] in technological design.

Most of the cast parts for transport and particular purpose types of diesel are made by casting method, which should be based on manufacturing's technological aspects, namely various casting defects [3]. These defects occur due to the lack of methods and tools to influence the technological modes of production. The design documentation and technical specifications usually specify the size and number of various casting defects that are not allowed in part, which means that such defects affect its quality and reliability.

The diesel's central part under consideration is a block-case, the quality of which will depend on the required characteristics laid down at the design stage. According to the technical conditions, requirements for the quality and reliability of cast parts of internal combustion engines are laid and fulfilled at the production stage using methods for determining technological defects [4].

Obtaining a high-quality block crankcase at the casting stage consists of two main processes: pouring molten metal into the mold and forming the cast part during the phase transition during cooling and crystallization.

2 Literature Review

The relevance of computer-integrated technologies for manufacturing parts occupies an essential place in the world. For many years, computer systems (CAE, CAD, and CAM) have been used to increase production productivity [5].

The most crucial advantage of computer-integrated technologies is that they emphasize the advanced capabilities of engineering analysis. For example, based on the finite element method [6]. The most striking feature of CAD/CAM systems is the so-called solid-state creation (modeling) of the product exclusively on the computer screen, viewing on the screen (visualization) of the process of processing parts and transmitting the generated data over computer networks to the CNC equipment [7].

Computer modeling becomes an integral part of designing new parts and designing technological processes for their manufacture. It acquires the status of an essential and often decisive competitive advantage. Increasingly, customers for foundry products in the list of requirements for the manufacturer of these products put forward a need for the mandatory use of computer modeling.

In a market economy, improving product quality and reducing metal and energy consumption is an urgent task. Consequently, the latest technologies are introduced in the production using computer modeling programs, which improves the quality of products without special costs for energy, metal, etc.

The advantages of automated modeling systems for foundry processes are described in many works [8, 9]. The main advantage is the ability to work out the nuances of casting technology on a virtual prototype of the cast, which reduces or eliminates the need for the production of test castings, reduces the process of designing the technology, and reduces the cost of casting [10]. The research work [11] shows that the visualization of physical processes foundry technology, such as the filling melt the mold cavity, cooling and solidification of metal warping under the action of thermal stress allows a better understanding of these processes, and therefore better manage them for reducing scrap in molding and increase yield.

Full-scale CAD/CAM/CAE systems are complex multifunctional systems that include a large set of modules (from 40 to 50) for various functional purposes [12].

In practice, various specialized and universal CAD/CAE/CAM systems of various versions and configurations are in operation in most enterprises. Very often, different strategies are used in divisions of the same organization. Sometimes this is even the case at the level of individual developers.

In the application of design of cast parts of modern systems (CAD/CAM/CAE/PDM and CIM), it is possible to provide [13]:

- Reduce production time and increase competitive products and output. Due to programs that provide speed for creating 3D models, regardless of the time spent on producing drawings on paper [14, 15];
- They can also provide significant cost savings. By using a software package that reduces the number of ongoing changes that accompany any design process, as well as errors [16];
- Improving the vibration reliability [17] and quality of manufacture. With the help of effective analysis of the created products, it can be tracked related defects in some software packages [18];
- It will allow you to design and produce better models [19] continuously;
- Maximum error elimination. Due to the visualization of the designed product, which allow us to eliminate typical errors in production promptly [20];
- Introduction of newer and more modern methods that allow us to develop productive strategies of 3D model design, as well as their visualization, consideration of fill processes, as well as possible defects [21];
- Avoiding large-scale layout products will reduce the time to create a specific part [22].

Modern design in foundry production includes developing a 3D model of a part, casting system, and equipment. The processes that occur must be consistent with practical methods that allow getting high-quality parts with higher performance characteristics [23].

The purpose of this work is to analyze the quality of cast block crankcase using a universal technology of complex computer- integrated design of cast parts of internal combustion engines using engineering modeling of thermal and hydrodynamic parameters of casting. Computer modeling of casting processes occurring in the manufacture of a cast part of the block crankcase is performed to identify the places of formation of defects, determine their location and estimated size, as well as for subsequent analysis of the phase transition process when cooling the casting of the block crankcase in the form.

3 Research Methodology

For achieving this objective, the following sequence of stages was proposed, according to the method of computer modeling of thermal and hydrodynamic casting processes:

- determination of the initial conditions;
- development of a 3D casting model based on a 4DTNA1 diesel block crankcase with a technological gating-feeding system;
- computer-integrated modeling of foundry processes for the production of cast block crankcase;
- analysis of the results of computer simulation;
- study of the nature of filling the mold with metal and the location of casting defects.

A cast 4DTNA1 diesel crankcase was selected as the studied part for computer-integrated modeling (Fig. 1).

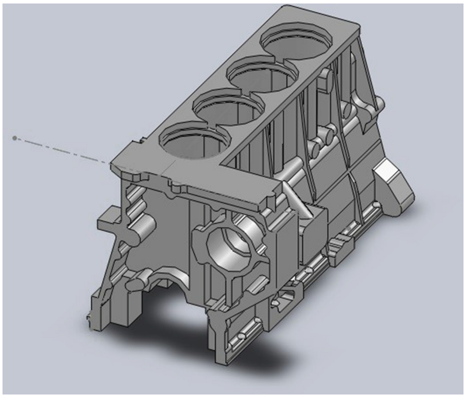

Fig. 1. Cast block crankcase of 4DTNA1 diesel.

A 3D model of block crankcase casting with a technological gating-feeding system was created in the ICS SolidWorks (Fig. 2). The gating-feeding system created is a "tapering type" system that ensures by its design the correct and gradual filling of the form with metal to avoid the ingress of slag inclusions into its cavity.

The boundary conditions and initial data for modeling according to the following sequence were set:

- 3D import (converting a file to *.stl format) and creating a finite-difference model;
- the purpose of the material for casting and tooling, as well as the separation coating, applied to the surface of the tooling;
- setting the initial temperature of the melt and process equipment, and cooling with various heat carriers;
- setting the total production cycle time for a single casting.

Using the 3D import module built into the ICS NovaFlow, the block crankcase model with a gating-feeding system and the equal model were converted into a finite-volume model.

The optimal cell parameters are set based on the calculation time-adequacy of the results (Fig. 2). The cell size is 3.7 mm.

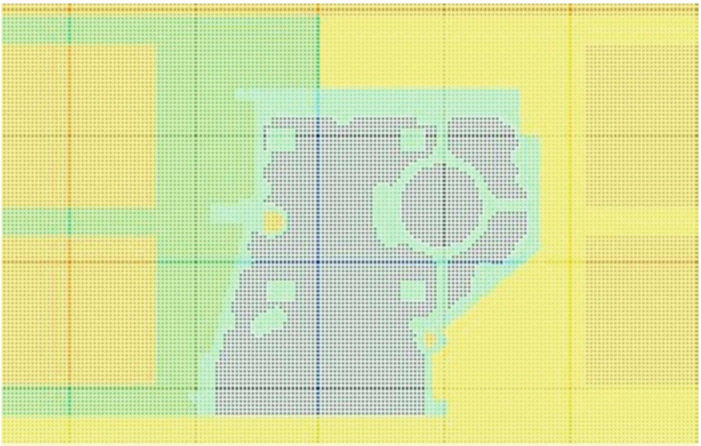

Fig. 2. Final-volume model of the casting in the chill with the displayed cells.

The assignment of boundary conditions for the material of casting elements and technological equipment is made by dividing into separate parts, each of which is given its color:

- block crankcase casting material is AlSi5Cu1Mg;
- materials of technological equipment are Steel 20, Grey Cast Iron 20;
- The chill forms are coated with chill paint with a thickness of 0.2 mm, which has a thermal conductivity of $\lambda = 0.3$ W/m*K.

To prevention moisture from entering the forming surface and a high-temperature difference when pouring, the process equipment was preheated to $T = 523 \div 553$ K.

The melt temperature before pouring into the mold was 983 K.

4 Results

The obtained results of computer-engineering modeling are presented graphically in filling the mold with a melt, the direction of crystallization during cooling (transition from the liquid to the solid phase), and displaying the location of gas-shrinkable defects.

The filling in the form plays an essential role in creating favorable conditions for directed crystallization. The velocity of the melt movement when filling the mold in separate parts did not exceed the critical values of $V_{kr} > 0.8$ m/s, with a smooth filling of the mold, without splashes, and with small vortices according to the requirements [17] (Fig. 3).

The results of computer simulation analysis showed that the movement of the melt in the mold could be considered as satisfying the following requirements:

- passing through the elements of the gating system, the melt does not acquire a turbulent character of movement;

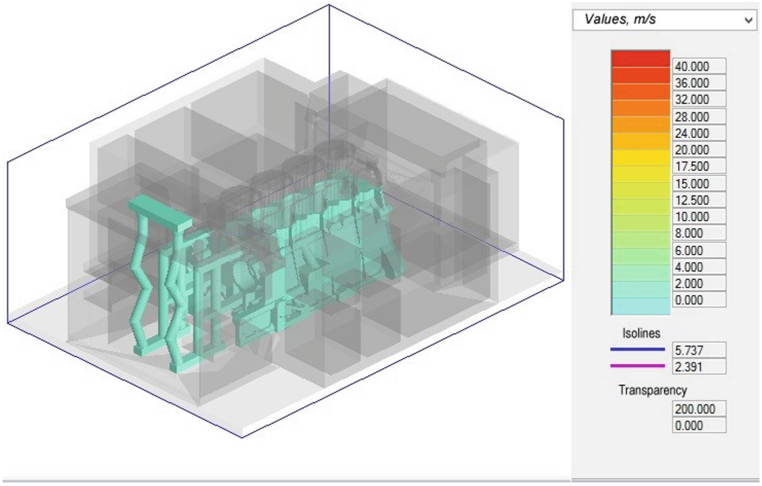

Fig. 3. General view of filling the form with melt.

- the mold is filled in without exceeding critical speeds.

The analysis of the results of computer-integrated simulation of the cooling process of the part in the technological mold (chill) was carried out under the parameters:

- the transition from the liquid to the solid phase during cooling of the part in the form (Fig. 4);
- gas-shrinkage defects expressed by the Niyama criterion [24] (Fig. 5).

Analysis of the dynamics of cooling of the casting, the phase transition, the connectivity of the zones that crystallize last allowed to determine the places of the possible occurrence of gas-shrinkable defects.

The conclusion is based on the analysis of the location of defects expressed in the ICS NovaFlow by the Niyama criterion.

The criterion for determining the location of gas-shrinkable defects and their magnitude is Niyama, which we use to predict microporosity and gas-shrink porosity large enough to be detected by radiographic testing. This criterion is a reliable predictor of porosity for simple castings. Still, in the case of castings with complex geometries, its use requires a more thorough analysis of the simulation results since many factors affect the formation of gas-shrink porosity.

Analysis of the locations of defects showed that the most prone to shrinkage places are:

- edge cavities of the cylinders;
- the upper plane in the front part of the block, in the places of attachment under the head;
- arrays of bosses on the sides of the block.
- Modeled defects allow us to forecast that the cast product may be defective by 5–6%.

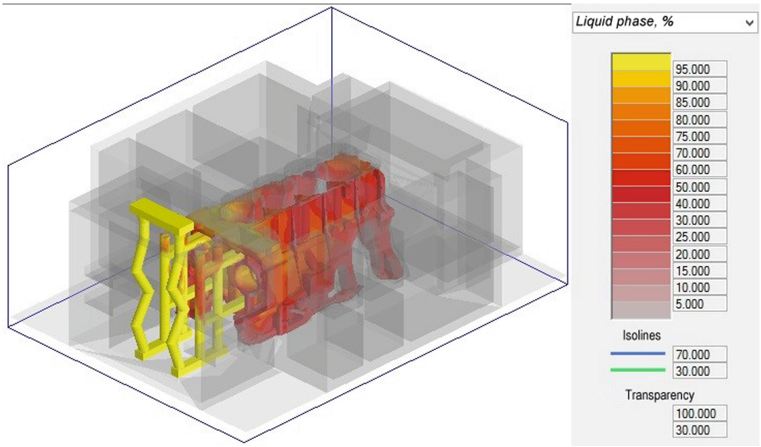

Fig. 4. The transition from the liquid to the solid phase during the cooling of the part in the chill.

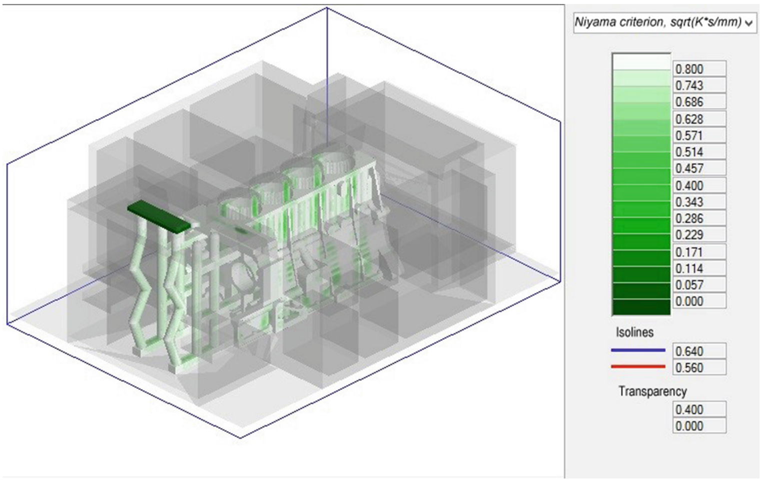

Fig. 5. Locations of gas shrinkage defects according to the Niyama criterion.

From the results of computer-engineering modeling of thermal and hydrodynamic processes of block crankcase casting, it follows that gas-shrinkage defects can be stress concentrators in the part's structural elements. Therefore, it can affect the strength characteristics during operation.

5 Conclusions

The developed 3D model of block crankcase casting with a technological gating-feeding system allowed creating a finite-difference model of casting and tooling and performing engineering modeling of casting processes in the ICS NovaFlow. The analysis of physical features of the processes of filling and cooling the castings in the form was performed for the cast block crankcase of 4DTNA1 automobile diesel, the locations and sizes of gas-shrinkable defects were determined according to the Niyama criterion.

The research results allowed us to form boundary and initial conditions for modeling the stress-strain state of the block crankcase in the places where gas-shrink porosity is formed.

Further development of the above studies will be carried out for castings of new types, configurations, other casting technologies, newly synthesized alloys.

References

1. Mehrabi, M.G., Ulsoy, A.G., Koren, Y.: Reconfigurable manufacturing systems: key to future manufacturing. J. Intell. Manuf. **11**, 403–419 (2000). https://doi.org/10.1023/A:1008930403506
2. Pavlenko, I., Trojanowska, J., Ivanov, V., Liaposhchenko, O.: Parameter identification of hydro-mechanical processes using artificial intelligence systems. Int. J. Mechatron. Appl. Mech. **2019**(5), 19–26 (2019)
3. Prasad, R.: Progress in investment castings. In: Science and Technology of Casting Processes. IntechOpen (2012)
4. Thomas, D.S., Gilbert, S.W.: Costs and cost effectiveness of additive manufacturing. NIST Spec. Publ. **1176**, 12 (2012). https://doi.org/10.6028/NIST.SP.1176
5. Milchev, G., Miltchev, R.: Development of information technologies, planned obsolescence and modification of the life-cycle of the CAD/CAM/CAE systems. Eur. J. Sustain. Dev. **7**(3), 217 (2018). https://doi.org/10.14207/ejsd.2018.v7n3p217
6. Rao, S.S.: The Finite Element Method in Engineering. Butterworth-Heinemann (2017)
7. Sang, Z., Xu, X.: The framework of a cloud-based CNC system. Procedia CIRP **63**, 82–88 (2017). https://doi.org/10.1016/j.procir.2017.03.152
8. Kumar, V., Madan, J.: A system for computer-aided gating design for multi-cavity die-casting dies. Proc. Inst. Mech. Eng. Part B: J. Eng. Manuf. **231**(11), 1983–1999 (2017). https://doi.org/10.1177/0954405415614727
9. Khan, M.A.A., Sheikh, A.K.: A comparative study of simulation software for modelling metal casting processes. Int. J. Simul. Model. **17**(2), 197–209 (2018). https://doi.org/10.2507/IJSIMM17(2)402
10. Kozłowski, J., Sika, R., Górski, F., Ciszak, O.: Modeling of foundry processes in the era of Industry 4.0. In: Ivanov, V., et al. (eds.) DSMIE. LNME, pp. 62–71. Springer, Cham (2019). https://doi.org/10.1007/978-3-319-93587-4_7
11. Bianchi, M.F., Gameros, A.A., Axinte, D.A., Lowth, S., Cendrowicz, A.M., Welch, S.T.: On the effect of mould temperature on the orientation and packing of particles in ceramic injection moulding. J. Eur. Ceram. Soc. **39**(10), 3194–3207 (2019). https://doi.org/10.1016/j.jeurceramsoc.2019.03.049
12. Ng, C.B.R.: A concurrent design facility architecture for education and research in multi-disciplinary design of complex systems (2019)
13. Wang, X., Bi, Z.: New CAD/CAM course framework in digital manufacturing. Comput. Appl. Eng. Educ. **27**(1), 128–144 (2019). https://doi.org/10.1002/cae.22063
14. Akimov, O., Soloshenko, V., Kostyk, K.: Computer-integrated design of cast parts on the criterion of performance on the example of the turbine wheel turbocharger. In: CEUR Workshop Proceedings, vol. 2353, pp. 324–338 (2019)

15. Akimov, O.V., et al.: Computer engineering and design of cast parts for internal combustion engine crankcase. J. Eng. Sci. **6**(2), E24–E30 (2019). https://doi.org/10.21272/jes.2019.6(2).e4
16. Dhahad, H.A., Alawee, W.H., Marchenko, A., Klets, D., Akimov, O.: Evaluation of power indicators of the automobile engine. Int. J. Eng. Technol. **7**(4.3), 130–134 (2018)
17. Pavlenko, I., Ivanov, V., Kuric, I., Gusak, O., Liaposhchenko, O.: Ensuring vibration reliability of turbopump units using artificial neural networks. In: Trojanowska, J., Ciszak, O., Machado, J.M., Pavlenko, I. (eds.) MANUFACTURING 2019. LNME, pp. 165–175. Springer, Cham (2019). https://doi.org/10.1007/978-3-030-18715-6_14
18. Boboulos, M.A.: CAD-CAM & Rapid Prototyping Application Evaluation. Bookboon (2010)
19. Kumar, S.L.X.: State of the art-intense review on artificial intelligence systems application in process planning and manufacturing. Eng. Appl. Artif. Intell. **65**, 294–329 (2017). https://doi.org/10.1016/j.engappai.2017.08.005
20. Laurel, B.: Design Research: Methods and Perspectives. MIT Press (2003)
21. Otto, K.N.: Product design: techniques in reverse engineering and new product development (2003)
22. Khan, M., Khan, S.S.: Data and information visualization methods, and interactive mechanisms: a survey. Int. J. Comput. Appl. **34**(1), 1–14 (2011)
23. Parsons, J.L., Campbell, J.R.: Digital apparel design process: placing a new technology into a framework for the creative design process. Cloth. Text. Res. J. **22**(1–2), 88–98 (2004). https://doi.org/10.1177/0887302X0402200111
24. Ignaszak, Z.: Discussion on usability of the niyama criterion for porosity predicting in cast iron castings. Arch. Foundry Eng. **17**(3), 196–204 (2017). https://doi.org/10.1515/afe-2017-0115

The Contact Pressure in Drawing Parts Without Clamping the Workpiece Flange

Roman Arhat[1](✉), Ruslan Puzyr[2], Viktor Shchetynin[1], Viacheslav Puzyr[1], and Tetiana Haikova[1]

[1] Kremenchuk Mykhailo Ostrohradskyi National University, 20, Pershotravneva Street, Kremenchuk 39600, Ukraine

[2] Kremenchuk Mykhailo Ostrohradskyi National University College, 7, Chumatskyi Shliakh Street, Kremenchuk 39621, Ukraine

Abstract. In the paper, dependence has been obtained to calculate the contact pressures when drawing down the axisymmetric workpiece without a blank flange collet. The solution is based on the assumptions of the momentless theory of shells. The adequacy of the mathematical model is confirmed by experimental data for a narrow interval of forging blanks. The experiments have been carried out on a specially designed tooling to measure load cell deformation using a strain gauge. All the equipment used has passed metrological control. To calculate the meridional and tangential stresses on the torus-shaped portion of the matrix, dependencies were obtained that contain a term connecting the thickness of the workpiece with the value of the stresses arising during drawing, which more accurately describes their distribution on the drawing edge of the matrix. The expression for calculating the surface contact pressure during the drawing of a cylindrical part makes it possible to consider the friction stresses at the radius of the matrix rounding and calculate the drawing force. The obtained dependence differs from the conventional ones in its simplicity and clarity and can be used at the preliminary stage of choosing equipment for stamping. It is shown that the friction stresses between the contacting surfaces can be controlled over a wide range while achieving a significant change in the stress state and the distribution of deformations in the volume of the workpiece.

Keywords: Metal drawing · Plastic deformation · Die body radius · Drawing punch · Contact pressure

1 Introduction

Drawing of axisymmetric parts is characterized not only by the loss of flange part stability but also by the deformation localization in the zone of the transition of the wall to the bottom and the destruction of the workpiece given location [1, 2]. The destruction and localization of deformations can be eliminated by reducing the tensile stress value. When drawing down with a collet, this problem is solved by reducing the collet force, using highly effective lubricants, and also polishing the die body contact surfaces and the blank holder [3–5].

V. Ivanov et al. (Eds.): DSMIE 2021, LNME, pp. 12–20, 2021.
https://doi.org/10.1007/978-3-030-77719-7_2

2 Literature Review

The drawing down without workpiece flange pressing is limited by the formation of workpiece uncompressed part. The bottom separation can occur if the process of workpiece retraction into the die body hole continues, ignoring the folds on the flange. As shown in the papers [6, 7], it is possible to extend the interval of non-collet forging by increasing the resistance of the flange, loss of stability, or increasing tensile stresses in the initial stage of deformation. The blank flange practically does not contact the surface of the die body, since when the punch is lowered, the flange portion rises above the die body and forms a conical surface with an angle α at the apex [8–11]. Therefore, the contact of the workpiece with the die body occurs along its toroidal surface with a certain rounded radius. The stresses in the drawn metal, the force, the drawing coefficient, and the corrugation and destruction of the blank depending on the radius of curvature of the drawing edge of the matrix [6, 12]. Therefore, it is chosen very carefully in each specifically selected technological process [3, 13]. The existing analytical dependences for calculating stresses at the radius of curvature do not fully consider all the minute details and technological factors of the drawing process, and their accuracy is not satisfactory [14, 15]. The presence of refined formal dependencies describing the distribution of stresses on the drawing edge of the matrix, taking into account friction, bending moments, contact pressure, blank thickness, and others, will make it possible to expand the range of drawn products without pressing the flange and reduce rejects to a minimum. Therefore, it is of great scientific interest to theoretically determine the contact stresses on the torus-shaped section of the matrix and the factors that make it possible to control the value of these stresses to find conditions for expanding the possibilities of drawing without a folding holder. This will enable finding more accurate theoretical dependences for calculating and analyzing the stress field when drawing cylindrical parts.

3 Research Methodology

To determine the contact stresses, we start from the equilibrium equations for the torus [6, 16], but taking into account the surface load

$$\left.\begin{array}{c}\frac{\partial R_2 N_1}{\partial \phi}+\frac{\partial((R_1 \sin\theta)T)}{\partial\theta}-N_2\frac{\partial R_2}{\partial\phi}+T\frac{\partial R_1\sin\theta}{\partial\theta}=0,\\ \frac{\partial((R_1\sin\theta)N_2)}{\partial\theta}+R_2\frac{\partial T}{\partial\phi}-N_1\frac{\partial(R_1\sin\theta)}{\partial\theta}+T\frac{\partial R_2}{\partial\phi}=0,\\ \frac{N_1}{R_1}+\frac{N_2}{R_2}=q.\end{array}\right\} \tag{1}$$

where N_1, N_2, T – are internal meridional, tangential, and shear stresses;

q – is the contact pressure.

We take into account the fact that the deformation is axisymmetric, and therefore the terms of the system (1) containing $\partial\phi$, as well as the shearing force T, and that $R_1 = \frac{R}{\sin\theta} = \frac{a(1+k\sin\theta)}{k\sin\theta}$, $R_2 = a$, $k = \frac{a}{R}$, then we will have [5, 17]:

$$\left.\begin{array}{c}N_2 a\cos\theta+\frac{\partial N_2}{\partial\theta}\frac{a}{k}(1+k\sin\theta)-N_1 a\cos\theta=0,\\ \frac{N_1\sin\theta}{R}+\frac{N_2}{a}=q.\end{array}\right\} \tag{2}$$

Next, we calculate according to the procedure [8, 18, 19] with the only difference that the pressure on the workpiece when it slides along the edge of the die body is applied from within half a torus.

where R_d – is the radius of the drawing part;

r_m The radius of the die body input edge; $R = R_d + a \sin\theta$; $a = r_m$.

When the torus is affected by a surface load with loss of stability in the form of bulge formation, the expression for q has been obtained by the authors of [8, 20, 21] as $k \to 0$:

$$q = \frac{E}{12\left(1-\mu^2\right)}\left(\frac{s}{a}\right)^3\left(n^2-1\right), \tag{3}$$

where μ – is Poisson's ratio;
E – is Young's modulus;
n – is the number of emerging half-waves with loss of stability.

Regarding our drawing conditions, it should be slightly modified. For further calculation, we use the cylindrical rigidity of the shell corresponding to the secant modulus $D \approx D' = \frac{E_c s^3}{9}$, we sort out the value of n for which $\left(n^2-1\right) = 1$. Further, since $E_c = \frac{\sigma_i}{\varepsilon_i}$, we accept $\sigma_i = \sigma_{cp}$, and $\varepsilon_i = \frac{1}{2}\varepsilon_\theta$ [22, 23]. The draw ratio is $m = \frac{D}{D_0}$, hence $\varepsilon_\theta = 1 - m = 1 - \frac{D}{D_0}$, where D and D_0 are the diameter of the workpiece and the diameter of the blank, respectively. Then expression (6) will have the form:

$$q = \frac{2\sigma_s}{9\left(1-\frac{D}{D_0}\right)}\left(\frac{s}{r_m}\right)^3. \tag{4}$$

We substitute this relation into the formulas for the internal forces and, passing to the stresses, we get:

$$\sigma_\rho = \frac{\sigma_s}{9\left(1-\frac{D}{D_0}\right)}\left(\frac{s}{r_m}\right)^2, \tag{5}$$

$$\sigma_\theta = -\frac{1+\frac{k}{2}\sin\theta}{1+k\sin\theta}\frac{2\sigma_s}{9\left(1-\frac{D}{D_0}\right)}\left(\frac{s}{r_m}\right)^2. \tag{6}$$

Formerly [6, 24], formulas were derived from calculating the magnitude of the stress tensor components on the torus-like part of the die body without considering the surface load. Using the principle of superposition [16, 25] and carrying out simple transformations, the final dependencies for calculation of meridional and tangential stresses on the rounded radius of the die body at θ = *90º* will look like:

$$\sigma_\rho = \sigma_s\left(\ln\frac{R_0}{R_d + r_m} - \frac{r_m}{R_d + r_m} + 0,1\frac{R_0}{R_0 - R_d}\left(\frac{s}{r_m}\right)^2\right), \tag{7}$$

$$\sigma_\theta = -\sigma_s\left(1 - \ln\frac{R_0}{R_d + r_m} + \frac{r_m}{R_d + r_m} + 0,22\frac{1+\frac{k}{2}}{1+k}\frac{R_0}{R_0 - R_d}\left(\frac{s}{r_m}\right)^2\right). \tag{8}$$

In contrast to correlations [6, 26], to calculate the meridional and tangential stresses on the torus-like part of the die body, the dependences (7) and (8) contain a term that relates the thickness of the blank to the value of the stresses arising while drawing, which describes their distribution on the drawing edge of the die body more accurately.

Below there are stress graphic dependences (Fig. 1) – the blank thickness for $R_0 =$ 50 mm, $R_d = 25$ mm and matrix rounding radius $r_m = 10$ mm, created according to formulas (7), (8).

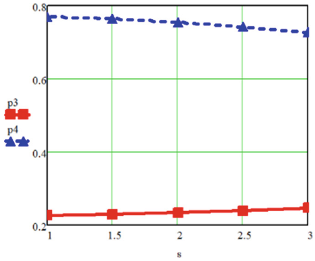

Fig. 1. Stress graphs (σ/σ_s) – the blank thickness (s), created according to dependences (7), (8).

Using the second system Eq. (2), as well as (10) and (8) and carrying out simple transformations, we find the surface pressure, which causes the plastic deformation of the blank during drawing without workpiece collet:

$$\frac{q}{s} = \sigma_s \left(\begin{array}{c} \left(\ln \frac{R_0}{R_d + r_m} - \frac{r_m}{R_d + r_m}\right) \frac{R_d}{(R_d + r_m)^2} \\ + \frac{R_0}{R_0 - R_d} \left(\frac{s}{r_m}\right)^2 \left(\frac{1}{9(R_d + r_m)} - \frac{2}{9r_m} \frac{1 + \frac{k}{2}}{1 + k}\right) - \frac{1}{r_m} \end{array} \right). \tag{9}$$

We analyze the terms of the expression for given deformation parameters – $R_0 = 50$ mm, $s = 2$ mm, $R_d = 25$ mm and $r_m = 10$ mm. The first and second terms are of the same order of smallness and can be neglected with an error up to the third decimal place. Then the surface load is the following:

$$q = -\frac{s}{r_m}\sigma_s. \tag{10}$$

To verify the obtained dependence by determining contact pressures, experiments have been carried out to measure the load cell deformations caused by frictional forces. Experimental and theoretical studies demonstrate [13, 18, 27, 28] that the frictional stresses between the surfaces to be contacted can be controlled within wide limits while achieving a significant change in the stress state and the distribution of deformations in the volume of blank, which is of great importance for the production of high-quality workpieces using drawing down.

Since the flange of the workpiece practically does not contact with the mirror of the die body while drawing down without the blank holder, and friction occurs mainly along the rounded radius of the latter, it is of great interest to determine the frictional stresses and to study their effect on the occurrence of the loss of flange stability.

The experiments were carried out on a tensile machine of UME-10TM type with a force of 10 tf [14, 24, 29].

The experimental equipment appeared to be a special die body with an inlet of 50 mm and a set of punches with diameters of 49.3 mm; 46.4 mm; 49 mm, providing the drawing of blanks without thinning the stiffening plate of 08kp steel with a thickness of 0.15 mm, of aluminum A2 with a thickness of 1.4 mm and copper M4 of 0.25 mm correspondently. The dying body was installed on the lower traverse of the tensile machine. The exchangeable punches were on the upper traverse. Both traverses were equipped with clamping elements.

Special equipment appeared to be a dying body, with an insert for the drawing radius, which can be displaced in the direction of movement of the punch during drawing and the punch of a conventional design (Fig. 2) [15, 30, 31].

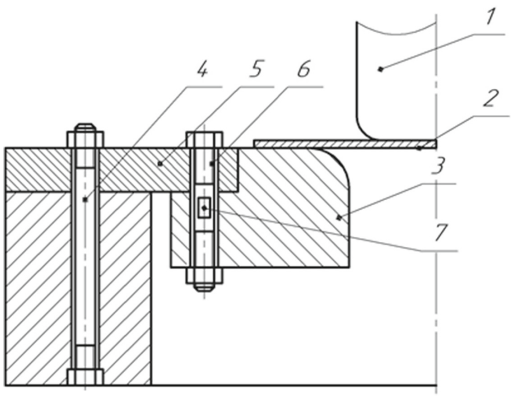

Fig. 2. Equipment for measuring frictional stresses at the rounded radius of the exhaust die body: 1 – punch; 2 – blank; 3 – movable insert; 4 – a fixing bolt; 5 – a connecting ring; 6 – load cell; 7 – strain gage.

The equipment for measuring the load cell deformations is a strain gauge operational amplifier MCP606-I/P, ADC E14–440, power supply unit AX-1803D and personal computer Pentium 4 CPU 2.40 GHz 1.0 GB RAM. Load cell deformations caused by frictional forces during drawing determined strain gages deformation, which is included in a quarter-bridge scheme without compensation of temperature stresses [32]. This, in turn, caused the change in the resistance of the resistor and the current in the circuit. The current oscillations were amplified by an operational amplifier and transmitted to the ADC. On the computer monitor, these current readings were recorded for a predetermined time. It was KF 5P1–5-200-A-12 strain gage, with an operating resistance of $R = 199.7 \pm 0.2\ \Omega$ and a base of 5 mm. The label of the resistors was produced with the "cyacrine" glue according to the technology described in the paper [33, 34].

4 Results

Thus, the contact pressure between the hemispherical surface of the die body and the workpiece was measured. Measurements were subjected to a minimum of 16 blanks for each metal and alloy with different coefficients of drawing. The load cell rounded radius $r_m = 4$ mm and $r_m = 1.5$ mm, without lubrication of the surfaces of the workpiece and the tool. Simultaneously, the depth of the punch's progress was recorded, such as force increase; a sharp force increase meant the occurrence of corrugations that made it difficult to draw a flat workpiece into the hole in the die. Based on the measurement results, typical ADC voltage-time charts are shown (Fig. 3). Also, the experimental data are used to verify the adequacy of the mathematical model of the distribution of contact pressures on the die body rounded radius when drawing without collet.

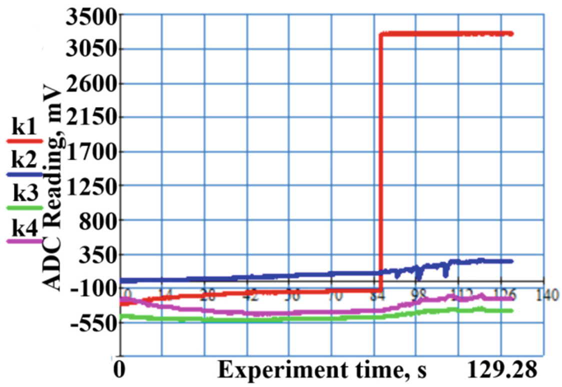

Fig. 3. A typical schedule of measurement of load cell deformations: k1 – the first load cell (breakage); k2 – the second load cell; k3 – the third load cell; k4 – the fourth load cell.

For greater accuracy of contact pressure measurements, the first lot of blanks was chosen in such a size that their diameter was equal $D_0 = D + 2r_m$, where D is the diameter of the drawing workpiece. This was to minimize the effect of blank flange deformation and reduce the impact of the bending moment on the torus-like section. The remaining two lots of blanks were selected with dimensions $D_0 = D + 4r_m$ and $D_0 = D + 6r_m$ correspondently. The results of the experimental data have been subjected to statistical processing [12, 35, 36], then averaged and summarized in Table 1. Processing experimental data on the measurement of contact pressures showed that their distribution is subjected to normal law at a significance level $q = 0.05$. The confidence error in the results of the experiment was assumed to be symmetric and amounted to $\Delta = \pm 0.26$ MPa.

In Table 1, in the numerator of the values of the diameter, the draw ratio, the stroke of the punch, the value of the contact pressure, which relate to the drawing option with the rounding radius of the die body $r_m = 4.0$ mm; in the denominator it is the same for $r_m = 1.5$ mm; Δ, % is deviations of the experimental data from the theoretical ones, calculated from the dependence (3).

Table 1. Results of experimental studies on the contact pressures measurement.

Material	Deformation parameters					Contact pressure	Estimated contact pressure	Δ, %
	s, [mm]	D_0, [mm]	k	r_m, [mm]	h, [mm]	q, [MPa]	q, [MPa]	
Steel 08kp	0.15	58/52 66/54 74/56	1.16/1.04 1.32/1.08 1.48/1.12	4/1.5 4/1.5 4/1.5	8.0/6.0 8.0/6.0 8.1/6.0	58/38 94/55 133/57	17.25/46.0	71.3/17.2 81.7/16.9 87.1/19.4
Aluminum A2	1.4	58/52 66/54 74/56	1.16/1.04 1.32/1.08 1.48/1.12	4/1.5 4/1.5 4/1.5	8.2/6.1 8.3/6.0 8.0/6.0	27/46 37/48 46/51	42/56	35.1/17.4 10.6/12.6 8.7/7.5
Copper M4	0.25	58/52 66/54 74/56	1.16/1.04 1.32/1.08 1.48/1.12	4/1.5 4/1.5 4/1.5	8.0/6.0 7.9/6.0 7.9/6.0	21/17 34/21 43/24	10/26.6	52.3/34.3 70.5/20.3 76.7/6.7

5 Conclusions

The results of experimental studies showed that the greatest coincidence with theory is 6.7% for drawing with $k = 1.12$ and $r_m = 1.5$ mm for copper and the greatest discrepancy in calculations is up to 87% for steel with $r_m = 4.0$ mm a rounded radius of the die body. The discrepancy between the results of experimental studies and calculated data in general can be explained by the imperfection of the mathematical model, where all factors of constructive and technological nature are not taken into account, as well as hardening of the metal during plastic deformation [37, 38]. The best coincidence between the results of theoretical and experimental studies, which does not exceed 20% (except copper drawing, $k = 1.04$, $r_m = 1.5$ mm), showed data for all metals with $r_m = 1.5$ mm. However, as can be seen from Table 1, an increase in the flange width results in an increase in the contact pressure, and the best coincidence of the results is observed precisely with the drawing of blanks with an enlarged flange. Therefore, the completion of the dependence is obvious. A further direction of research on this issue will concern its refinement in terms of considering the bending moments acting on the radius of the matrix rounding, which should result in greater adequacy of solutions.

References

1. Golovlev, V.: The initial stage of drawing sheet metal. Forging and stamping production. Mater. Work. Press. **7**, 4–10 (1995)
2. Kalyuzhnyi, O.: Intensification of forming processes of cold sheet stamping. Sik Group Ukraine LLC, Kyiv (2015)
3. Yan, G., Wang, X., Deng, L.: A study of hole flanging-upsetting process. Adv. Mater. Res. 939, 291–298 (2014). https://www.scientific.net/AMR.939.291
4. Luo, J.: Study on stamping-forging process and experiment of sheet metal parts with non-uniform thickness. Huazhong Univ. Sci. Technol. **51**, 45–54 (2011).

5. Gavas, M., Izciler, M.: Effect of blank holder gap on deep drawing of square cups. Mater. Des. **28**, 1641–1646 (2007)
6. Puzyr, R., Savelov, D., Argat, R., Chernish, A.: Distribution analysis of stresses across the stretching edge of die body and bending radius of deforming roll during profiling and drawing of cylindrical workpiece. Metall. Min. Ind. **1**, 27–32 (2015)
7. Popov, E.: Fundamentals of the theory of sheet punching. Engineering, Moscow (1977)
8. Volmir, A.: Stability of Deformable Systems. The Science, Moscow (1967)
9. Ogorodnikov, V.A., Dereven'ko, I.A., Sivak, R.I.: On the influence of curvature of the trajectories of deformation of a volume of the material by pressing on its plasticity under the conditions of complex loading. Mater. Sci. **54**(3), 326–332 (2018). https://doi.org/10.1007/s11003-018-0188-x
10. Salenko, Y., Puzyr, R., Shevchenko, O., Kulynych, V., Pedun, O.: Numerical simulation of local plastic deformations of a cylindrical workpiece of a steel wheel rim. In: Ivanov, V., et al. (eds.) DSMIE 2019. LNME, pp. 442–451. Springer, Cham (2020). https://doi.org/10.1007/978-3-030-50794-7_43
11. Yang, C., Li, P., Fan, L.: Blank shape design for sheet metal forming based on geometrical resemblance. Procedia Eng. **81**, 1487–1492 (2014)
12. Anishchenko, O., Kukhar, V., Grushko, A., Vishtak, I., Prysiazhnyi, A., Balalayeva, E.: Analysis of the sheet shell's curvature with lame's superellipse method during superplastic forming. Mater. Sci. Forum 945, 531–537 (2019).https://www.scientific.net/MSF.945.531
13. Borisevich, V., Zahirnyak, M., Drabobetsky, V.: Choosing the optimal parameters for extracting sheet blanks. Forging and stamping production. Mater. Work. Press. **2**, 38–41 (2009)
14. Sosenushkin, E., Yanovskaya, E., Sosenushkin, A., Emel'yanov, V.: Mechanics of nonmonotonic plastic deformation. Russ. Eng. Res. **35**(12), 902–906 (2015). https://doi.org/10.3103/S1068798X15120199.
15. Guo, Y., Batoz, J., Naceur, H., Bouabdallah, S., Mercier, F., Barlet, O.: Recent developments on the analysis and optimum design of sheet metal forming parts using a simplified inverse approach. Comput. Struct. **78**, 133–148 (2000). https://doi.org/10.1016/S0045-7949(00)00095-X
16. Sivak, R.: Evaluation of metal plasticity and research of the mechanics of pressure treatment processes under complex loading. East.-Eur. J. Enterp. Technol. **6/7**(90), 34–41 (2017). https://doi.org/10.15587/1729-4061.2017.115040
17. Anishchenko, A., Kukhar, V., Artiukh, V., Arkhipova, O.: Application of G. Lame's and J. Gielis' formulas for description of shells superplastic forming. MATEC Web of Conf. **239**, 06007 (2018). https://doi.org/10.1051/matecconf/201823906007
18. Ogorodnikov, V., Savchinskij, I., Nakhajchuk, O.: Stressed-strained state during forming the internal slot section by mandrel reduction. Russ. J. Heavy Mach. **12**, 31–33 (2004)
19. Leyu, W., Daxin, E.: Numerical simulation analysis of variable BHF drawing of rectangular cup on curve blank-holder. Mod. Manuf. Eng. **2**, 73–74 (2006)
20. Wang, X., Ouyang, K., Xia, J.: FEM analysis of drawing-thickening technology in stamping-forging hybrid process. Forg. Stamp. Technol. **34**(4), 73–78 (2009). https://doi.org/10.3969/j.issn.1000-3940.2009.04.017
21. Akbari-Mousavi, S., Barrett, L., Al-Hassani, S.: Explosive welding of metal plates. J. Mater. Process. Technol. **202**(1–3), 224–239 (2008)
22. Del', G., Tomilov, F., Ogorodnikov, V.: Stressed state during the hot extrusion of steel. Steel USSR **5**(4), 223–224 (1975)
23. Comsa, D., Banabic, D.: Numerical simulation of sheet metal forming processes using a new yield criterion. Key Eng. Mater. **344**, 833–840 (2007)

24. Puzyr, R., Haikova, T., Trotsko, O., Argat, R.: Determining experimentally the stress-strained state in the radial rotary method of obtaining wheels rims. East.-Eur. J. Enterp. Technol. **4**(1(82)), 52–60 (2016). https://doi.org/10.15587/1729-4061.2016.76225
25. Puzyr, R., Savelov, D., Shchetynin, V., Levchenko, R., Haikova, T., Kravchenko, S., Yasko, S., Argat, R., Sira, Y., Shchipkovakyi, Y.: Development of a method to determine deformations in the manufacture of a vehicle wheel rim. East.-Eur. J. Enterp. Technol. **4**(1(94)), 55–60 (2018). https://doi.org/10.15587/1729-4061.2018.139534
26. Renne, I., Ogorodnikov, V., Nakhaichuk, V.: Plotting plasticity diagrams by testing cylindrical samples in combined tension and torsion. Strength Mater. **8**(6), 733–737 (1976)
27. Mori, K., Nakano, T.: State-of-the-art of plate forging in Japan. Prod. Eng. Res. Devel. **10**(1), 81–91 (2015). https://doi.org/10.1007/s11740-015-0648-1
28. Zagirnyak, M., Drahobetskyi, V.: New methods of obtaining materials and structures for light armor protection. In: International Conference 2015, ICMT, vol. 1, pp. 705–710 (2015)
29. Ogorodnikov, V.A., Grechanyuk, N.S., Gubanov, A.V.: Energy criterion of the reliability of structural elements in vehicles. Mater. Sci. **53**(5), 645–650 (2018). https://doi.org/10.1007/s11003-018-0119-x
30. Harpell, E., Worswick, M., Finn, M., Jain, M., Martin, P.: Numerical prediction of the limiting draw ratio for aluminum alloy sheet. J. Mater. Process. Technol. **100**, 131–141 (2000). https://doi.org/10.1016/S0924-0136(99)00468-9
31. Del, G., Ogorodnikov, V., Nakhaichuk, V.: Criterion of deformability of pressure shaped metals. Notification High. Educ. Inst. Mech. Eng. **4**, 135–140 (1975)
32. Zagirnyak, M., Kalinov, A., Ogar, V., Lotous, V.: Experimental assessment of the accuracy of the method for determination the power on an induction motor shaft. In: 18th International Conference 2017, CPEE (2017). https://doi.org/10.1109/CPEE.2017.8093054
33. Markov, O., Zlygoriev, V., Gerasimenko, O., Hrudkina, N., Shevtsov, S.: Improving the quality of forgings based on upsetting the workpieces with concave facets. East.-Eur. J. Enterp. Technol. 5/1(95), 16–24 (2018). https://doi.org/10.15587/1729-4061.2018.142674
34. Kukhar, V., Yelistratova, N., Burko, V., Nizhelska, Y., Aksionova, O.: Estimation of occupational safety risks at energetic sector of Iron and Steel Works. Int. J. Eng. Technol. (UAE) **7**(2), 216–220 (2018). https://doi.org/10.14419/ijet.v7i2.23.11922
35. Markov, O.E., Perig, A.V., Zlygoriev, V.N., Markova, M.A., Kosilov, M.S.: Development of forging processes using intermediate workpiece profiling before drawing: research into strained state. J. Braz. Soc. Mech. Sci. Eng. **39**(11), 4649–4665 (2017). https://doi.org/10.1007/s40430-017-0812-y
36. Anishchenko, A., Kukhar, V., Artiukh, V., Arkhipova, O.: Superplastic forming of shells from sheet blanks with thermally unstable coatings. In: MATEC Web of Conference, vol. 239, p. 06006 (2018). https://doi.org/10.1051/matecconf/201823906006
37. Sotiria, H., Spyros, A.: Stability of long transversely-isotropic elastic cylindrical shells under bending. Int. J. Solids Struct. **47**, 10–24 (2010). https://doi.org/10.1016/j.ijsolstr.2009.09.004
38. Logesh, K., Raja, V., Krishnan, D., Azeemudeen, M., Andrew, A., Hariprasath, K.: Experimental investigation and analysis of tensile and forming behaviour of cold rolled sheet metal. Int. J. Mech. Eng. Technol. (IJMET) **8**(11), 252–264 (2017)

Complex Recognition Approach for Cutting Part of Cutters in Finishing Turning

Oleksandr Derevianchenko(✉) and Oleksandr Fomin

Odessa National Polytechnic University, 1, Shevchenko Avenue, Odessa 65044, Ukraine
algdrv@opu.ua

Abstract. In the conditions of finishing and precision turning, the traditional approach to laboratory assessment of the condition of cutters by periodically recording the parameters of the wear zone along the flank surface and subsequent recognition is, in the authors' opinion, insufficiently effective. It does not consider significant changes (due to wear) in the geometry of the cutting edges and, in particular, in the forming of their sections, the state of which directly affects the quality of the processed surface. Therefore, there is a need for complex control and complex recognition of cutting part states. The article aims to develop an approach to complex recognition of cutters cutting part in finishing turning. The scientific novelty consists of creating classifiers for complex recognizing the states of cutters for finishing turning, using the most informative features of the shape of all wear zones, and analyzing their effectiveness. The research was carried out under conditions of processing hardened steel 115CrV3 on a lathe model TPC - 125 BH1P. On a special laboratory stand, equipped with a vision system, comprehensive periodical monitoring of the condition of the cutting part of the cutters for finishing was carried out. Practical usefulness consists of developing a method for predicting the residual life of cutters for finishing turning, using a set of features characterizing the shape and size of defects and microdefects of all wear surfaces of the cutting part. Timely replacement of a failed tool with a new one provides a significant economic effect.

Keywords: Tools failures · States of cutters · Complex of classifiers

1 Introduction

In the conditions of finishing and precision turning, the traditional approach to laboratory assessment of the condition of cutters by periodically recording the parameters of the wear zone along the flank face and subsequent recognition is, in the authors' opinion, insufficiently effective.

Nowadays, in cutting tools (CT) technical diagnostics, a trend is being developed based on smart diagnostic systems. These systems can create, compare, and transform CT models of a given subject area to make decisions based on accumulated knowledge and without the operator's participation in this process. The cutting part (CP) of any CT is characterized by a certain structure and geometry determined by the tasks required

V. Ivanov et al. (Eds.): DSMIE 2021, LNME, pp. 21–30, 2021.
https://doi.org/10.1007/978-3-030-77719-7_3

by the processing results. We can say that the working part of the cutting edge (CE) is a variable structure system. It does not take into account significant changes (due to wear) in the geometry of the cutting edges and, in particular, in the forming section of the CE, the state of which directly affects the quality of the processed surface. Therefore, there is a need for complex control and complex recognition of CP states.

The connection of the wear zones of the flank and rake face leads to significant gradual changes in the shape and geometry of the working sections of the CP.

The development carried out was focused on recognizing the states of the worn flank face of tools. However, in finishing and precision machining conditions, it is also necessary to recognize the rake surface and CE conditions.

2 Literature Review

The 5G technology in the next future will have a major impact on the industry [1]. This will enable manufacturers to complete end-to-end automation with the virtual deployment of new product lines or the entire factory. 5G will enable growth and transformation in Industry 4.0. In production conditions of Industry 4.0 became an actual new technological process. For example, in [2] is proposed progressive manufacturing process, based on the concept of intensification of machining and application of multiaxis equipment. It made the possibility to reduce the complexity of the manufacturing process (in drilling, milling, and boring operations).

One major challenge is designing the strategy for communication between the factory modules and the identification of adequate communication technologies [3].

Now the tasks of intelligent forecasting of the operability of modern technical systems are becoming relevant. For example, deep learning model creation is used for predicting the remaining useful life of the machining tools [4].

An artificial neural network model is developed to predict the main cutting force, and its ability to predict cutting force was analyzed in [5]. An effort is made to optimize the cutting parameters to accomplish minimum cutting force using a genetic algorithm. In work [6] features, obtained by processing the cutting force, vibration signal, and surface texture of the machined surface in turn, which are found by tool condition monitoring, are used to estimate cutting tools states.

Cutting tool failure in the manufacturing industry causes damage to the cutting tools; leads to serious accidents [7]. So, a wear monitoring system is required to mitigate these negative effects in the metal cutting manufacturing process. More and more diverse mathematical models are beginning to be used in the metalworking industry when creating mathematical and software for monitoring systems of machine tools and tools. In particular, the application of discrete and continuous Markov chains is promising [8].

It is especially noteworthy is the development of new promising strategies in CAD / CAM systems [9] and their use in diagnostic and monitoring systems for modern automated manufacturing [10].

An important role in data collections and modern computing technology are playing cloud computing and cloud manufacturing (CM) [11–13]. CM as a new technological paradigm has been attracted a large amount of research interest. When solving various diagnostic problems, such intelligent technologies as pattern recognition [14–16], the formation of statistical classifiers [15], digital image processing [14, 17], and others are increasingly used. They will begin to find application for building classifiers and recognizing the states of cutting tools (CT) [11, 14]. In the publication [11], we show the prospects for using cloud technologies and creating a central laboratory for the development of classifiers of instrument states based on the use of direct and indirect control methods. Therefore, the need to develop an approach to complex recognition of the states of the cutting part (CP) of worn-out tools is obvious.

The article aims to develop an approach to complex recognition of cutting parts of cutters in finishing turning.

3 Research Methodology

The experimental research was carried out under conditions of processing hardened steel 115CrV3 on a lathe model TPC - 125 BH1P. On a special laboratory stand, equipped with a vision system (Fig. 1), comprehensive periodical monitoring of the condition of the cutting part of the cutters for finishing was carried out. Digital images of CP wear zones were recorded. The formation of signs and recognition of the states of the flank faces is discussed in detail in our work [11]. Therefore, the main attention is paid to determining the signs of the states of the CP rake face and cutting edges. For cutting part states recognizing and of the CT residual life predicting – is shown on Fig. 1.

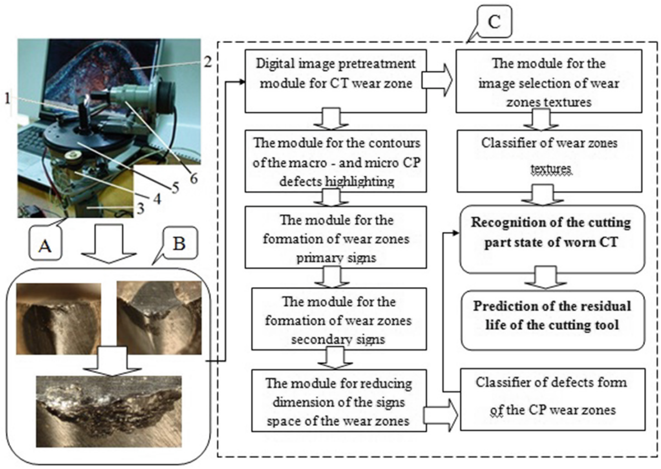

Fig. 1. Fragment of a smart system for cutting part (CP) states recognizing and of the CT residual life predicting.

The scheme contains 3 functional zones (A, B, C). In zone A, a fragment of the stand is shown for sequential monitoring of the wearing tool. The stands main elements: 1–CT; 2–a digital image of the wear zone of the rake face on the monitor screen; 3–control system fundament; 4–table rotation mechanism; 5–turntable on which the controlled tool is mounted; 6–digital camera. If necessary, it provides registration of many digital panoramic CP images, which can form a 3D - CP model.

In zone B, some of the samples of CT images in different projections are shown. They are the source data for obtaining the primary signs of the shapes and textures of the CP wear zones. Zone C represents a fragment of the of smart system intellectual component. Zone C shows the sequential operations of complex processing and analysis of images for each worn surface. Due to the limitations of the volume of the article, we will consider only some of them.

4 Results

Consider fragments of the image processing of the front surface of a worn CNB cutter after wearing CT monitoring. (Fig. 2). In the resulting image 1, a fragment of the wear zone 2 (crater wear) is selected with subsequent scaling (3). After its conversion to binary (4), wear zone contour (5) is selected, and feature sets are formed (6, 7).

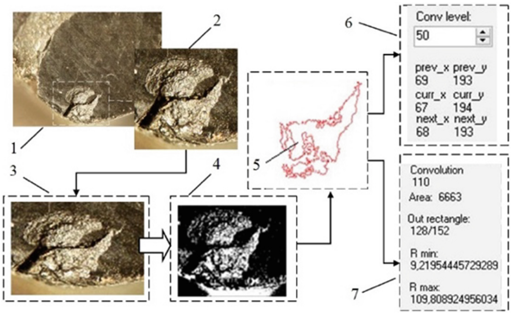

Fig. 2. Fragments of the image processing of the rake face with the crater wear of a worn CNB cutter.

In the structure of the process of complex recognition of the states of worn CT of cutters for finishing, an important place belongs to recognizing the states of the cutting edges. The representation of the classes of form changes of the CT in the process of wear of the cutting part is shown in Fig. 3.

When registering digital images of the rake face of the CT in the initial state $(\hat{R}^{\tau_0}_{CE})$ and the state of wear$(\hat{R}^{\tau_1}_{CE})$ - zone 1 - as a result of the processing $\mu^{\tau_0}_{CE}$ of the binary image (2), there is a selection (3) of the CE contours of the new $(\overline{R}^{\tau_0}_{CE})$ and worn (not shown in Fig. 3) cutter. The combination of these contours gives the contours of the displacement of the CE as a result of wear.

Several classes of these contour shapes are highlighted (in position 1 is shown the class Ω_1). At the bottom of Fig. 3 schematically shows the combined projections of the CE on the main plane $(R^{\tau_0}_{CE}, R^{\tau_1}_{CE}, R^{\tau_2}_{CE}, R^{\tau_3}_{CE})$ for the moments of processing τ_1, τ_2, τ_3 (the shaded outline corresponds to the class Ω_1).

In the structure of Fig. 3 indicates the coordinate system $\hat{Y}\hat{X}$, in which the projections are combined, and the coordinate system $X(D_S)$, Y, where is the vector D_S of movement of the cutter feed. Complex contour shapes are caused by the formation of grooves on the CT rear surface. Attention should be paid to the sequential change in the positions

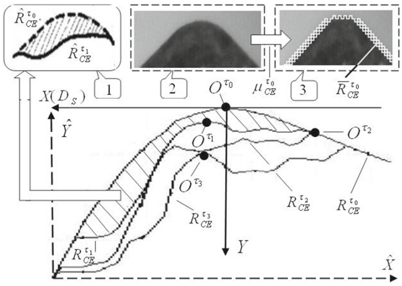

Fig. 3. Representation of the classes of form changes of the CE in the process of wear of the cutting part (fragment).

of the points of the tops (O^{τ_0}-O^{τ_1}-O^{τ_2}-O^{τ_3}), which is due to the radial wear of the CT. Recognition of classes of contours (Ω_1–Ω_5) is a component of the complex recognition of the state of the CT source. Let's move on to some of the CP defects and microdefects. In Fig. 4 shows images of zones of concentrated wear of the flank face (1), the groove-notch wear (2), and the lowering section of the cutting edge (3).

The following parameters are determined from such images: h_{CE} the amount of lowering (CE displacement) due to the closure of wear zones, the groove's height. Grooving and concentrated wear zones are common when machining hardened steels. The grooves weaken the cutting part of the CT and can cause its local destruction. Therefore, the growth of the parameter h_{GRV} is taken into account in the complex forecasting of the residual resource of the CT. With the formation of traces of concentrated wear on the forming section of the CE, the machined surface quality deteriorates sharply. Due to the closure of the wear zones on the front and rear surfaces, the effect of lowering the cutting edge section to a height h_{CE} and the formation of a small threshold on the front surface is formed.

When this parameter reaches the limit value, the chips stop coming off the rake face because they rest against the threshold and moves vertically upward. This prevents the chip breaking process; chips fill the treatment area, leading to an accident.

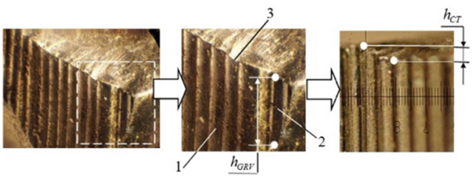

Fig. 4. Images of wear zones of the flank wear of the cutter with traces of defects.

This is especially true on flexible production modules. Therefore, the growth of the parameter h_{CE} is taken into account in the complex forecasting of the residual resource of the CT. The main results of the formation of classifiers are shown in Figs. 5, 6, 7, 8 and 9. Let's move on to a comparative analysis of the quality of classifiers for complex recognition of CP states.

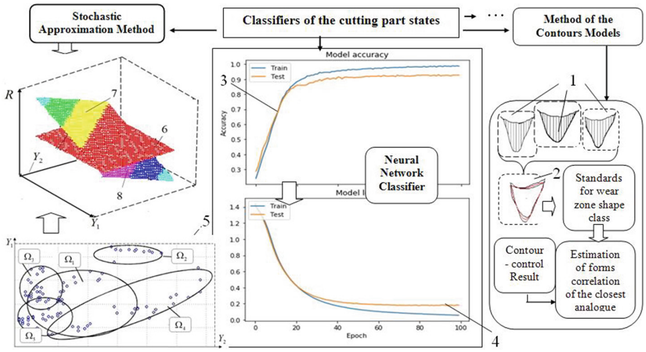

Fig. 5. Some results of a comparative analysis of the quality of classifiers for complex recognition of CP states.

Here 1 is a set of contours of the flank wear zones recorded under the same processing conditions; 2 - reference contour (shape class), formed as a result of processing set 1; 3, 4 - respectively, graphs of changes in the accuracy of the neural network on the training and examination samples; 5 - an example of the intersection of regions of 5 classes of states of the flank wear cp; positions 6–8 show an example of the work of the classifier generated by the stochastic approximation method (6 - classifier; 7 – class 1; 8 - class 2). Figure 5 demonstrated the scheme of classifiers set, which can be used in the experiments. Classifiers were built using the method of contours models of wear zones (1, 2), stochastic approximation method, and neural networks. In cases where the probability density functions of the diagnostic features in the training set are known, the stochastic approximation method (SAM) is effectively used. However, in practice, and especially in the production environment, such estimates are not accurate or completely absent. In this case, a device of neural networks can give a good result. The results of computational experiments show that even simple neural networks created using Python (a programming language) and Keras (libraries for constructing and training neural networks) demonstrate a high recognition quality of CT states. An example of using the Python programming language and the Keras library to build a neural network-based cutting tool state classifier is presented below (Fig. 6). The algorithm includes the following steps: 1. Import of required modules and libraries; 2. Loading the training data set; 3, dividing the training sample into training and examination; 4. Neural network training with Keras; 5. Train the neural network with executing code; 6. I am checking the accuracy of the training data; 7. They are obtaining the conclusion.

The process of neural network training (for recognizing classes of states of the worn back face of the cutters CP) is presented in Fig. 7. After 100 training epochs (it will take around a minute), the training accuracy is reached 94.5% (Fig. 7) - so the model is trained.

In a wide range of external conditions, the use of genetic algorithms becomes justified. The results of computational experiments using the Python programming language and the Deap library of genetic algorithms - demonstrate the fast and effective construction of diagnostic features space of minimum dimension (Fig. 8). So, from a set of 8 primary signs, the algorithm selected 4 of the most informative ones. This base CT

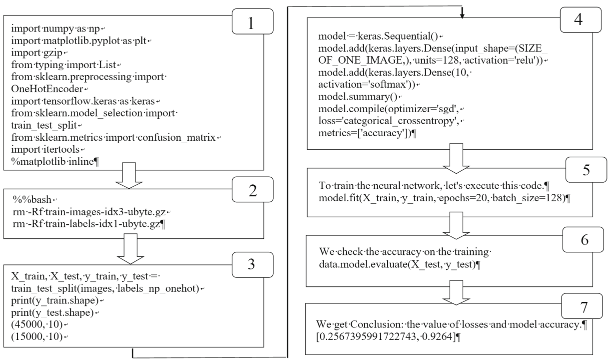

Fig. 6. An example of using the Python programming language and the Keras library to build a neural network-based cutting tool state classifier.

model is constructed in the form of a neural network, which provides the recognition quality of CT states of 98.5%, so the preference is given to the neuron set method. Let's move on to the analysis space of signs and predict CT residual life (Fig. 9).

After receiving the secondary signs of wear zones, internal and external micro defects (traces of concentrated wear, groves at the cut layer borders, the appearance of lowering sections of the CE, etc.), process formation of the Y attribute space occurs.

In this conditionally multidimensional CP state space, the areas of the tool state classes are displayed (Ω_1, Ω_2, Ω_3). Class Ω_1 - incisors are worn flank wear surfaces without visible micro-defects. In this class, at the control moments τ_1, τ_2, two states (c_{τ_1}, c_{τ_2}) are identified, which correspond to feature vectors (y^{τ^1}, y^{τ^2}).

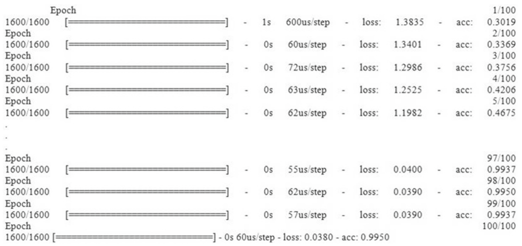

Fig. 7. The neural network training (for recognizing classes of states of the worn back face of the cutters CP).

The indicated states of the cutter differ in the size of the flank wear zone. The wear process is conventionally depicted by $W^{(\tau_1-\tau_2)}$. Further CT wear ($W^{(\tau_2-\tau_3)}$, $W^{(\tau_3-\tau_4)}$) leads to the appearance of new wear zones traces of concentrated wear; section of lowering the cutting edge (due to the closure of the wear zones). They are significant in finishing (class Ω_2) - state c_{τ_3}, c_{τ_4} (a digital image corresponding to the state c_{τ_4}, is given conditionally here).

```
kom deap import base
from deap import creator
from deap import tools
POP_SIZE = 8
creator.create("FitnessMax",
base.Fitness, weights=(1,))
creator.create("Individual",
str, fitness=creator.FitnessMax)
toolbox = base.Toolbox()
toolbox.register("attr_str",
generate_random_words, n=1)
ind = creator.Individual
(toolbox.attr_str())
pop = [creator.Individual
(toolbox.attr_str()) for _
in range(POP_SIZE)]
print(ind)
print(pop)
RESULTS: - [2, 3, 6, 8]
```

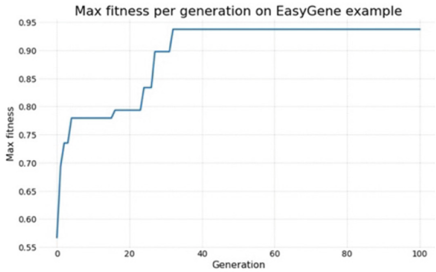

a. b.

Fig. 8. Features space selection using genetic algorithm.

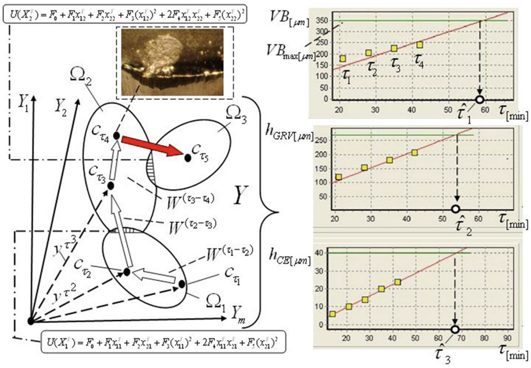

Fig. 9. Schema of the cutter states changing (as it wears out) in the space of signs and complex prediction of its residual life.

Pay attention to the fact that there is an intersection of class areas $\Omega_1, \Omega_2, \Omega_3$ (shaded areas). In this case, the use of the SAM becomes an alternative. The corresponding classifiers (sets of decision rules - separating hypersurfaces $((U(X1), U(X2)))$ are polynomials of the 2nd degree.

The right part of Fig. 9 shows the prediction schemes for the residual life of the cutter (with the conditional use of a linear model) according to four parameters ($VB_{[\mu m]}$; $h_{GRV[\mu m]}$; $h_{CE[\mu m]}$). Hire: $h_{GRV[\mu m]}$ - groove height; $h_{CE[\mu m]}$ - CE lowering value. Green lines indicate the limit values of each parameter. From the obtained values of the time period for the loss of CT workable state ($\hat{\tau}_1$; $\hat{\tau}_2$; $\hat{\tau}_3$), the smallest is selected. The prediction result is transmitted to the CNC system.

5 Conclusions

The smart system has been developed for complex recognizing states and predicting the residual life of a cutting tool. A special laboratory stand was tested for direct monitoring of CT states using vision systems; image processing of wear zones ensured the formation of sets of CT states signs. A number of wear zones ststateigns were obtained, which were used to form the corresponding classifiers. We tested 3 types of CT state classifiers constructed using SAM, method of contours models of wear zones, and neural networks. The related software packages have been developed using the programming languages Python and Keras library. The best results were shown by the neural network classifier, which will be used in further studies.

The dimensionality of the CP states space reduced using genetic algorithms. From a set of 8 primary signs, the algorithm selected 4 of the most informative ones. The cutting state's models were constructed in the form of a neural network, which provides the probability of correctly recognizing CT states of 98.5%.

In future investigations, authors planning to create fuzzy – neuron classifier for CT states complex recognition (to provide 100% quality of state recognition).

References

1. Peraković, D., Periša, M., Zorić, P., Cvitić, I.: Development and implementation possibilities of 5G in Industry 4.0. In: Ivanov, V., Trojanowska, J., Pavlenko, I., Zajac, J., Peraković, D. (eds.) DSMIE 2020. LNME, pp. 166–175. Springer, Cham (2020). https://doi.org/10.1007/978-3-030-50794-7_17
2. Ivanov, V., Dehtiarov, I., Zaloga, V., Kosov, I., Savchuk, V.: Increasing productivity of connecting rods machining. In: Ivanov, V., Trojanowska, J., Pavlenko, I., Zajac, J., Peraković, D. (eds.) DSMIE 2020. LNME, pp. 264–275. Springer, Cham (2020). https://doi.org/10.1007/978-3-030-50794-7_26
3. Mukku, V.D., Lang, S., Reggelin, T.: Integration of LiFi technology in an Industry 4.0 learning factory. Procedia Manuf. **31**, 232–238 (2019). 9th Conference on Learning Factories, Braunschweig, Germany
4. Liu, C., Zhang, L., Niu, J., Yao, R., Wu, C.: Intelligent prognostics of machining tools based on adaptive variational mode decomposition and deep learning method with attention mechanism. Neurocomputing **417**, 239–254 (2020)
5. Leo Dev Wins, K., Anuja Beatrice, B., Ebenezer Jacob Dhas, D.S., Anita Sofia, V.S.: Artificial neural network and genetic algorithm-based models for predicting cutting force in turning of hardened H13 steel. In: Vijayan, S., Subramanian, N., Sankaranarayanasamy, K. (eds.) Trends in Manufacturing and Engineering Management. LNME, pp. 627–635. Springer, Singapore (2021). https://doi.org/10.1007/978-981-15-4745-4_56
6. Cheng, M., Jiao, L., Shi, X., Wang, X., Yan, P., Li, Y.: An intelligent prediction model of the tool wear based on machine learning in turning high strength steel. J. Eng. Manuf. **234**(13), 1580–1597 (2020)
7. Marani, M., Zeinali, M., Kouam, J., Songmene, V., Mechefske, C.K.: Prediction of cutting tool wear during a turning process using artificial intelligence techniques. Int. J. Adv. Manuf. Technol. **111**(1–2), 505–515 (2020). https://doi.org/10.1007/s00170-020-06144-6
8. Olekh, T., Gogunskii, V.: Use of discrete and continuous markov chains for system absorbing states. In: 2019 IEEE International Conference on Advanced Trends in Information Theory, ATIT 2019 - Proceedings, pp. 518–521 (2019)
9. Dodok, T., Cubonova, N., Cisar, M., et al.: Utilization of strategies to generate and optimize machining sequences in CAD/CAM. In: 12th International Scientific Conference of Young Scientists on Sustainable, Modern and Safe Transport Location: High Tatras. Procedia Engineering, vol. 192, pp. 113–118 (2017).
10. Kuric, I., Císar, M., Tlach, V., Zajačko, I., Gál, T., Więcek, D.: Technical diagnostics at the department of automation and production systems. In: Burduk, A., Chlebus, E., Nowakowski,

T., Tubis, A. (eds.) ISPEM 2018. AISC, vol. 835, pp. 474–484. Springer, Cham (2019). https://doi.org/10.1007/978-3-319-97490-3_46

11. Fomin, O., Derevianchenko, O.: Improvement of the quality of cutting tools states recognition using cloud technologies. In: Ivanov, V., Trojanowska, J., Pavlenko, I., Zajac, J., Peraković, D. (eds.) DSMIE 2020. LNME, pp. 243–252. Springer, Cham (2020). https://doi.org/10.1007/978-3-030-50794-7_24
12. Liu, Y., Wang, L., Vincent Wang, X.: Cloud manufacturing: latest advancements and future trends. In: 8th Swedish Production Symposium, pp. 62–73. Waterfront Convention Centre Stockholm, Sweden (2018). Procedia Manuf.
13. Newman, S.T., Nassehi, A., Xu, X.W., Rosso, R.S.U., Wang, L., Yusof, Y., et al.: Strategic advantages of interoperability for global manufacturing using CNC technology. Robot. Comput.-Integr. Manuf. **24**(6), 699–708 (2008)
14. Antoshchuk, S., Derevianchenko, O., Tkachenko, E.: The hierarchical objects analysis on images of cutting tool wear zones. In: International Conference TCSET 2006 Conference Proceedings. pp. 253–255 (2007)
15. Vapnik, V.: The Nature of Statistical Learning Theory. Springer, Heidelberg (2013)
16. Aivazjan, S., Buxshtaber, V., Enjukov, I., Mechalkin, L.: Applied statistics. Classification and dimension reducing. Finance and Statistics, Moscow (1989). (in Russian)
17. Jahne, B.: Digital Image Processing. Springer, Heidelberg (2005)

Fractal Analysis of Structural and Phase Changes in the Metal of Welded Steam Pipe Joints

Yaroslav Garashchenko(✉), Alyona Glushko, Olena Kobets, and Olena Harashchenko

National Technical University "Kharkiv Polytechnic Institute", 2, Kyrpychova St, Kharkiv 61002, Ukraine

Abstract. The research results of the ability to assess the boundaries of structural components' geometric complexity, which are visible in a metallographic analysis of the metal samples of Welded Steam Pipe Joints, considering the operating time, are presented. The estimation of the complexity of grain boundaries was made based on a statistical analysis of fractal dimensions obtained by the cellular method for measuring the grain boundary length. The fractal analysis of microsection images is carried out using a developed program. The computer system was tested for several samples cut from sections of steam pipelines with different operating times, operated under conditions of creep and low-cycle fatigue. A comparative analysis of fractal dimensions of structural components' boundaries in the microsections images of various metal sections with different operating times is carried out. The research and comparative analysis are carried out for the heat-affected zone, base metal, weld, and substrate areas. As a result, the possibility of assessing the complexity of the boundaries of structural components in the steam pipelines metal and their welded joints was confirmed based on the analysis of statistical characteristics of the distribution of their fractal dimension.

Keywords: Metallographic analysis · Boundaries of structural components · Geometrical complexity · Fractal dimension

1 Introduction

Structural changes in the steam pipelines metal made of heat-resistant pearlitic steel 12Cr1MoV (analog of steel 14MoV6-3, 1.7715 EN 10216-2:2020), which are operated under conditions of creep and low-cycle fatigue, lead to a deterioration in their properties. Identifying premature degradation processes in metal by forming defects based on metallographic analysis of structural changes is essential to ensure a trouble-free operation of steam pipelines [1].

The use of fractal analysis is one of the approaches for quantifying metallographic images. It is known that the fractal dimension of metallographic image components can be used as a characteristic of the fatigue of metal polycrystals [2]. The fractal dimension of a metal's structural components is an effective quantitative characteristic

V. Ivanov et al. (Eds.): DSMIE 2021, LNME, pp. 31–40, 2021.
https://doi.org/10.1007/978-3-030-77719-7_4

of the process of self-organization of the material structure during fatigue. It depends on the initial structure of the material and the duration of cyclic loads [2].

2 Literature Review

The development of methods for assessing the materials structure and modern computer technologies has brought to a new level the ability to carry out their quantitative assessment [3]. The metal structure is represented by space-filling irregular elements [4]. The correlation between parameters of the metal structure and their physical and mechanical properties has been studied by many authors [5, 6]. The presence of an element of subjectivity in assessing the metal structure lies in the fact that many of its elements, due to their complex configuration, are difficult to quantitatively describe [7]. This fact leads to the loss of important information about the "structure-property" tandem. The structure's geometric description is usually presented at the following three levels [4]: qualitative, quantitative, and topographic. The quantitative assessment of grain structures usually calculates the average grain size, grain boundary density, statistical grain size distribution, and porosity [7].

There is an approach that integrates 3D-modeling and visual analysis of metal structure [8]. Modeling produces valid polygonal 3D-representations of the structure by adopting a physics-based particle packing procedure.

Known studies [9] have shown that the self-organization model of metal structure can be used for cyclic actions. The specific features of the formation of microstructure and substructure [10] of metal under long-term cyclic influences in the form of dissipative structures make it possible to use the theory of fractals to describe them [11]. Fractal image analysis is used in many scientific fields [12, 13]. In materials science, fractal analysis is used to study the metal's microstructure since its structure can be interpreted as a fractal image [13, 14]. Fractal dimension and lacunarity are determined by the results of fractal analysis [11]. There are many methods for determining the fractal dimension for an image proposed in [15, 16]. Using these methods produces differing results. Comparative assessment of several methods is presented in [17].

The value of fractal dimension characterizes the quantitative parameters of structural elements and the physical properties of these elements' boundaries [10]. Determining the correlation between specified properties and fractal dimension of grain boundaries is a rather complicated but solvable problem [13].

This research shows a hypothesis about the statistical analysis of the fractal dimension distribution of the boundaries of selected structural components using the cellular measurement method, which will make it possible to scientifically determine their geometric complexity and consider this complexity when assessing the material structure effect on the properties and the residual resource.

The purpose of the research is to substantiate the assessment of boundaries complexity of the structural components of steam pipeline metal and its welded joints based on cellular method, considering the operating life.

3 Research Methodology

Analysis of metallographic images of metal samples of steam pipelines was carried out using statistical fractal analysis of images developed at NTU “Kharkiv Polytechnic Institute” (Ukraine). This system quantifies the metal structure based on the pixel array analysis using *RGB* and *HSV* color models. A subsystem has been developed to solve the problem and is shown in Fig. 1.

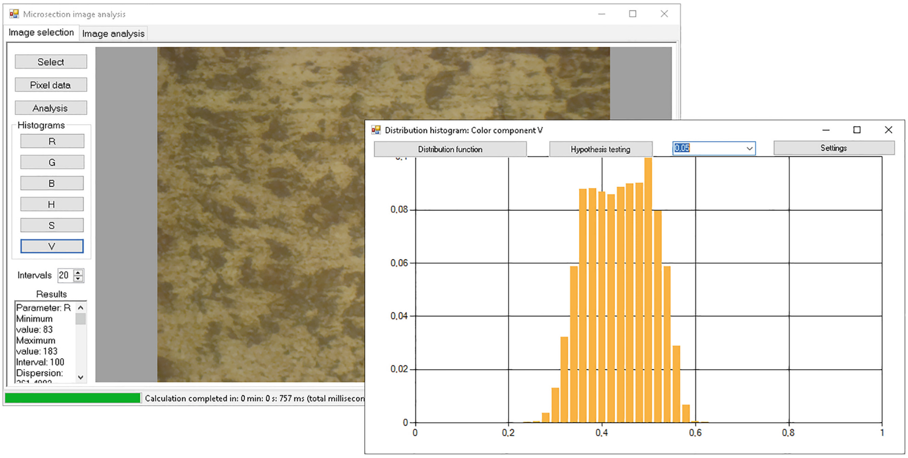

Fig. 1. Screen form of the fractal image analysis system.

This system (Fig. 1) gives a user the following basic capabilities:

- forming of pixels array with the definition of color components using *RGB* and *HSV* models;
- image visualization;
- determination of main statistical characteristics of color components distribution;
- determination of fractal dimension for a given range of scales (scaling area) to measure the length of the contour of selected pixels;
- statistical distribution analysis of the selected pixels over the width and length of the image;
- visualization of analysis results in the form of density or cumulative probability function.

The definition of RGB and HSV color model components for pixel array is performed by defining their properties: Red, Green, Blue, Hue, Saturation, Brightness (Value).

The research of possibilities of assessing the fractal dimension of boundary pixels was carried out using metallographic images of four samples of welded joints microsections cut from operating steam pipelines. One sample is taken as a baseline version, which has no operating time. For the rest of the samples, the operating time was 120 and 150

Table 1. Chemical composition of steel 12Cr1MoV (GOST 5520-79).

C, %	*Si, %*	*Mn, %*	*Ni, %*	*P, S, %*	*Cr, %*	*Mo, %*	*V, %*	*Cu, %*
0.08 ÷ 0.15	0.17 ÷ 0.37	0.4 ÷ 0.7	<0.3	<0.025	0.9 ÷ 1.2	0.25 ÷ 0.35	0.15 ÷ 0.30	<0.2

thousand hours. All samples' base material is heat-resistant pearlitic steel 12Cr1MoV (the chemical composition is presented in Table 1).

The scheme for determining the fractal dimension of selected image pixels in the developed system (Fig. 1) is shown in Fig. 2.

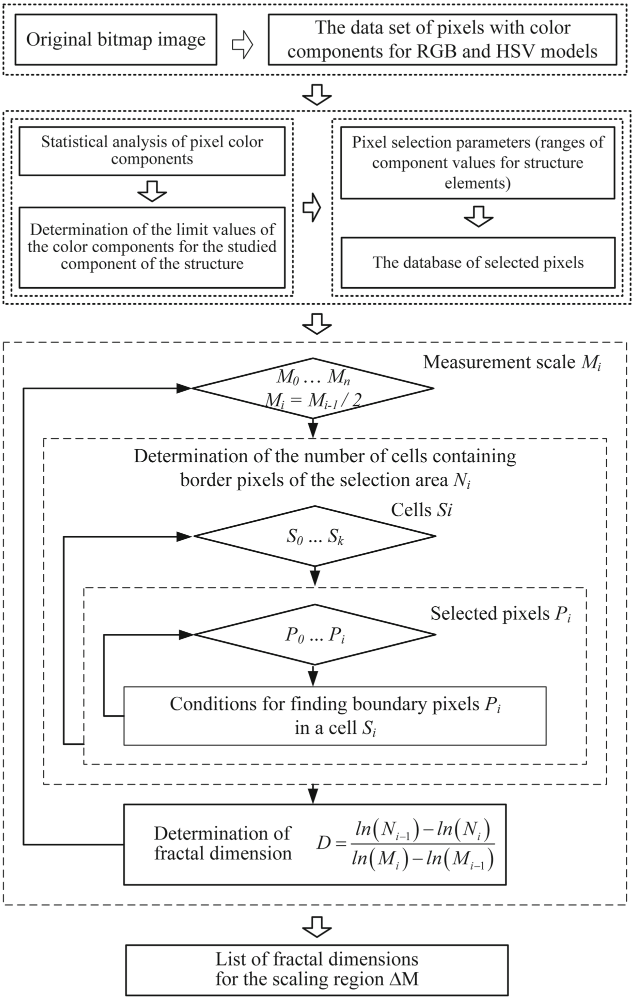

Fig. 2. Scheme for calculating the fractal dimension of selected image pixels.

The selection areas of metal structure elements in the microsection image (Fig. 1) are formed by setting the value range of selected RGB or HSV color components. Consequently, closed selection areas are formed consisting of an array of pixels related to the studied structural element. Such areas are obtained due to the values of pixel color components falling within a specific range. In most cases, selection regions are created based on a need to consider the structure's main component. For the contours of selection areas, we take the boundary selected pixels, defining the condition for the location of unselected pixels next to them (one or more that do not fall outside the specified cell). At the same time, the typical problem of fractal geometry to determine the length of a curved line using an array of cells with specified dimensions (which is called the "measurement scale" [7]) is quite applicable to the contours. Solving this problem is the coefficient of fractal dimension D of contour for a particular scaling area ΔM (range of cell sizes).

Given the theoretical background [18], fractal dimension D quantifies a contour's complexity (it contains border pixels) as a factor of change in detail with a change in scale. Fractal dimension is determined by the following formula [7]:

$$D = \frac{ln(N_{i-1}) - \ln(N_i)}{\ln(M_i) - \ln(M_{i-1})}, \qquad (1)$$

where M_i - measure (cell size) for the i-th measurement of the length of structural element boundaries under study; N_i is the number of scales (cells with size M_i) covering the contour (boundary pixels).

Coefficient D obtained by formula (1) can take a non-integer value, characterizing the degree of filling the image with the studied boundary pixels [19].

According to this scheme (Fig. 2), with a sequential change in the scale, the process of measuring the length of boundaries of selected areas of metal structure elements is repeated by several scales of N_i (cell size M_i) that cover entirely the boundary pixels [7] (Fig. 3 shows an example of microsection image with selected pixels). The pearlite zones' selection in the microsection image was carried out by replacing the original color (Fig. 3a) with white (Fig. 3b). As a threshold value of color brightness, $V_{max} = 0.46$ was visually selected to highlight perlite in the image of a metal microsection. This value is also seen in density function (brightness) component values V for the HSV color model.

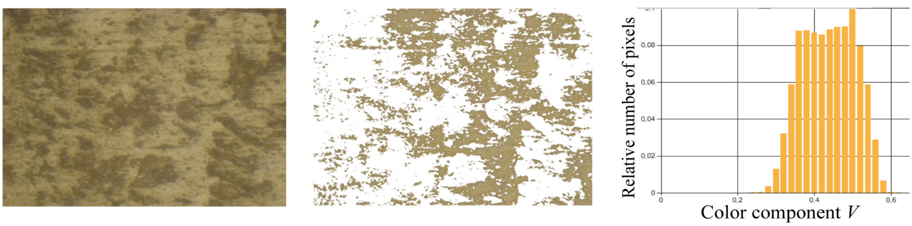

a *b* *c*

a - original image; *b* - image with selected pixels;
c - histogram of the *V* component (brightness) for the *HSV* color model

Fig. 3. Visual analysis of the microsection image of the weld metal without operating time.

As applied to the cellular method, a scale is called a cell (square) of size M. The scale should be significantly less than the measured contour length or a total number of boundary pixels ($M < < L$). In formula (1) number N will increase with decreasing value M (a more significant number of more minor scales are required to cover the boundary pixels fully).

Concerning a contour consisting of boundary pixels, its complexity and, accordingly, the fractal dimension will depend on the scaling area $\Delta M = M_{i-1} - M_i$. When measuring a real contour using a measure $M \rightarrow 0$, the length $L = const$. In this case, according to formula (1), the fractal dimension will correspond to the Euclidean dimension of the contour $D = 1$. If we consider increasing the image resolution (decreasing the pixel size $p_{image} \rightarrow 0$) applied to a perfectly etched sample, the contour length increases $L \rightarrow L_{ideal}$. Therefore, the fractal dimension of the contour obtained by the sequential arrangement of boundary pixels will always be $D \in (1, 2]$ (on condition that the cell size M does not exceed the contour size).

There are always restrictions on the minimum and maximum value of measurement scale M [20] in practice. In this study, the measurement scale's limitations will be the image size and the condition for determining the boundary pixel. Therefore, a cell with dimensions of 2×2 pixels will be the minimum acceptable. Accordingly, the initial measures M_i were chosen from the list $M_i = \{2, 4, 8, 16, 32, 64\}$ pixels (at image resolution - 1536×1152). The values of measures were set in a geometric progression with a common ratio $r = 2$. The number of contour length measurements was performed up to 5 times to obtain a wider scaling area of ΔM.

The studied images of microsections have the exact resolution. Accordingly, the use of specified M values for all images made it possible to obtain the fractal dimension's relative values, which can be compared. This circumstance makes it possible to carry out a comparative analysis of the studied grains' contours (boundary pixels) for all samples.

A separate study was carried out to substantiate the visually determined value of the brightness threshold V_{max} for the selected area of the microsections structural element. For this purpose, the fractal dimension of boundary pixels (the contour of the selected area) was determined depending not only on the measurement scale but also on the specified threshold V_{max}. 3D plot for $D = f(M, V_{max})$ is shown in Fig. 4 using the example of a steam pipeline weld with an operating time of 150 thousand hours.

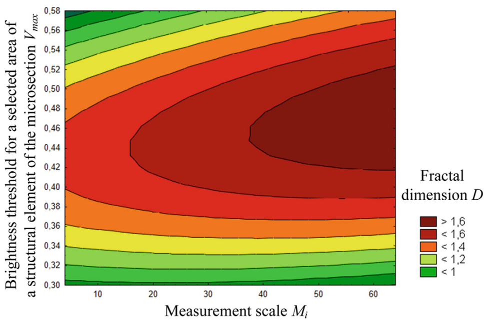

Fig. 4. Brightness threshold correlation for the selected area of the microsection structural element and the measurement scale with a fractal dimension of boundary pixels.

In the microsection image shown in Fig. 3, the main structural element is pearlite, which has the highest relative content in the metal. The main structural element's real boundary will be highlighted in the area of maximum fractal dimension and the largest measurement scale on graph $D = f(M, V_{max})$ (Fig. 4).

The largest fractal dimension is observed in the domain of the most significant values of measurement scale $M_i = 64$ pixels and $V_{max} = 0.46 \pm 0.04$ (Fig. 4). In this way, we confirm the correctness of value's (V_{max}) choice for the studied microsections component's contour (Fig. 3). This V_{max} value is correct for samples obtained under similar laboratory conditions.

4 Results

Results of calculations to determine the fractal dimension of selected components contours for microsections of test samples are shown in Fig. 5. The graph of the typical influence of measurement scale on the number of filled cells with boundary pixels is shown in Fig. 5a. This graph confirms the fractal analysis application's validity since it has a nearly linear relation of log-transformed characteristics $lg(N) = \lg(M)$. This relation is typical for fractal contours.

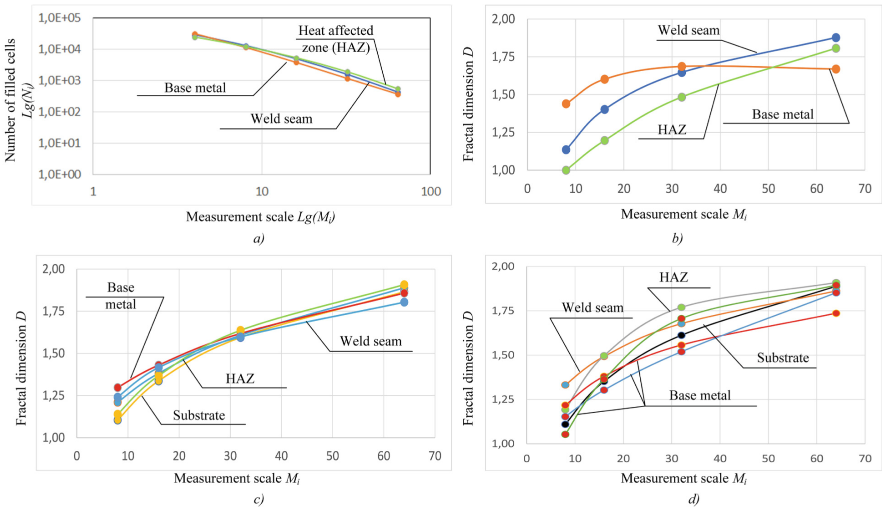

a - influence of the measurement scale on the number of filled cells with boundary pixels for a sample without operating time; *b, c, d* - the relationship between the measurement scale and the fractal dimension for samples with an operating time of 0, 120, and 150 thousand hours respectively.

Fig. 5. Results of fractal analysis of microsection images.

Figure 5 b-d shows the different options for the relation between the measurement scale and the microsection fractal dimension for steam pipeline samples. All dependencies are characterized by an increase in the fractal dimension with growth in the measurement scale. This case was separately studied by grouping the fractal analysis results by measurement scale (statistical analysis using the “Box Whiskers” swing chart is shown in Fig. 6.) Such a diagram shows general trends and significant differences in the ranges of fractal dimension values depending on the measurement scale. The greatest overlap of the fractal dimension domain was noted for the measurement scales $M_i = \{16, 8\}$ pixels. The smallest is for $M_i = \{32, 16\}$ pixels. In general, the results obtained do not contradict the well-known studies of the fractal dimension of contours or components of the metal structure [6, 12]. The most informative for assessing the steam pipeline residual resource can be considered the measurement scale $M_i = 8$, since the largest range of values of the fractal dimension D_i is observed.

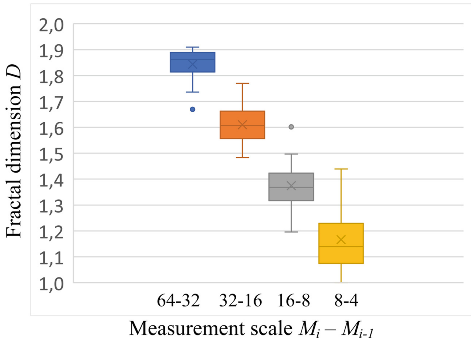

Fig. 6. Statistical analysis of the fractal dimensions of boundary pixels, grouped by measurement scale, regardless of operating time.

The statistical analysis of fractal dimensions grouped by metal sections (weld, base metal, heat-affected zone, and substrate) and the operating time is shown in Fig. 7. Heat-affected zone has the most extensive range of values according to experimental microsections D_i. For the initial sample (without operating time), the base metal has the smallest range of D_i values, which is entirely explainable due to the lack of influence of external factors on a metal structure.

There are identified trends. If for the initial sample arithmetic mean value $\overline{D_i}$ for the base metal is more significant compared with a weld and heat-affected zone, then with an increase in operating time, the opposite situation is observed, that is, a significant relative decrease in $\overline{D_i}$. There is also a growing trend of D_i for all areas under the study with an operating time. Therefore, with the operating time, the contours’ complexity for the tested element of metal structure increases. This feature is the most pronounced for the heat-affected zone. This feature’s study makes it possible to determine the residual resource of a steam pipeline.

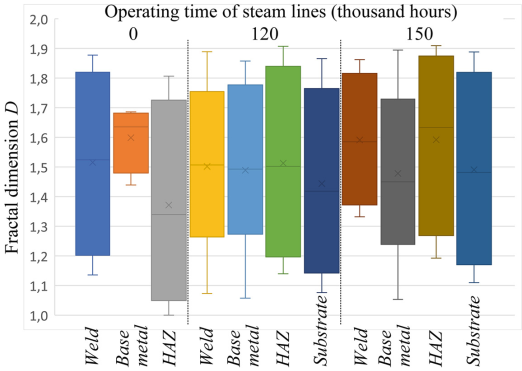

Fig. 7. Statistical analysis of the fractal dimensions of boundary pixels, grouped by metal sections and the operating time.

5 Conclusions

Statistical analysis of the distribution of fractal dimension of microsections of steam pipelines metal, obtained by the cellular method, makes it possible to scientifically determine grain boundaries' geometric complexity (areas of structural elements).

The original study of the effect of V_{max} and measurement scale M_i on the fractal dimension D_i carried out for the first time and made it possible to obtain a universal idea of the complexity of the contours of all structural components of the microsection image under study. The dependence $D_i = (V_{max}, M_i)$ made it possible to substantiate the threshold value of color brightness for studying the boundaries of pearlite, which is the structure's main component.

The influence of steam pipeline time on structural changes, expressed by an increase in fractal dimension and, accordingly, by the complexity of structural components contours, has been confirmed.

Further research is an analysis of the correlation between obtained data and the mechanical properties of the metal. This analysis will expand the possibilities for identifying structure parameters based on metallographic and fractal analyses and predicting a steam pipeline's residual resource.

References

1. Glushko, A.: Research into defectiveness of welded joints of steam pipes operated over a long time. East. Eur. J. Enterp. Technol. **6**(1 (84)), 14–20 (2016). https://doi.org/10.15587/1729-4061.2016.85852
2. Kuznetsov, P., Petrakova, K., Schreiber, Y.: Fractal dimension as a characteristic of fatigue of metal polycrystals. Phys. Mesomech. **7**(S1-1), 389–392 (2004)
3. Suryanarayana, C.: Microstructure: An Introduction. In: Prasad, E., Wanhill, R.J.H. (eds.) Aerospace Materials and Material Technologies. IIMS, pp. 105–123. Springer, Singapore (2017). https://doi.org/10.1007/978-981-10-2143-5_6
4. DeHoff, R.T.: Microstructology: the realistic and quantitative description of microstructural evolution. Metall. Microstruct. Anal. **1**, 244–258 (2012). https://doi.org/10.1007/s13632-012-0042-8

5. Dmytryk, V., Glushko, A., Tsaryk, A.: Recrystallization in the metal of welding joints of steam trucks. Prob. Atomic Sci. Technol. **5**, 49–52 (2019)
6. Miletić, I., Ilić, A., Nikolić, R.R., Ulewicz, R., Ivanović, L., Sczygiol, N.: Analysis of selected properties of welded joints of the HSLA steels. Materials **13**(6), 1301 (2020)
7. Bolshakov, V., Volchuk, V., Dubrov, Y.: Fractals in Materials Science, 1st edn. PGACA (2006)
8. Rodrigues, A.M., Bardella, F., Zuffo, M.K., Leal Neto, R.M.: Integrated approach for geometric modeling and interactive visual analysis of grain structures. Comput. Aided Des. **97**, 1–14 (2018)
9. Anisovich, A., Tovpenets, R.: Synergetic approach to describing structural changes during cyclic thermal effects. Eng. Phys. J. **75**(1), 15–20 (2002)
10. Tofpenets, P., Anisovich, A.: Possibility of using the fractal analysis to describe alloys' structures after pulse processing. Cast. Metall. **1**(37), 143–145 (2006)
11. Stoffel, A., Rabkin, M.: Use multifractal analysis to estimate the properties of structural steel. Metall. Mater. Sci. **10**(31), 24–27 (2016). [in Russian]
12. Moskvin, P., Balytska, N., Melnychuk, P., Rudnitskyi, V., Kyrylovych, V.: Special features in the application of fractal analysis for examining the surface microrelief formed at face milling. East. Euro. J. Enterp. Technol. **2**(1(86)), 1–7 (2017). https://doi.org/10.15587/1729-4061.2017.96403
13. Krivonosova, E.A., Krivonosova, E.K., Trushnikov, D.: Fractal geometry in metallurgy of welding and coatings. Mater. Sci. Forum **893**, 252–256 (2017)
14. Fernández, R., González-Doncel, G., Garcés, G.: Fractal analysis of strain-induced microstructures in metals. In: Fractal Analysis - Selected Examples (2020)
15. Li, J., Du, Q., Sun, C.: An improved box-counting method for image fractal dimension estimation. Pattern Recogn. **42**, 2460–2469 (2009)
16. Liu, J., Jiang, X., Huang, X., Shaohua, W.: Morphological characterization of super fine pulverized coal particle. Part 2. AFM investigation of single coal particle. Fuel **89**(12), 3884–3891 (2010). https://doi.org/10.1016/j.fuel.2010.07.001
17. Risović, D., Pavlović, Ž: Performance assessment of methods for estimation of fractal dimension from scanning electron microscope images. Scanning **35**(6), 402–411 (2013)
18. Albers, A., Gerald, A., Mandelbrot, B.: In His Own Words. Mathematical People: Profiles and Interviews. AK Peters, Wellesley (2008)
19. Falconer, K.: Fractal Geometry: Mathematical Foundations and Applications. Wiley, New York (2014)
20. Perrier, E., Tarquis, A., Dathe, A.: A program for fractal and multifractal analysis of two-dimensional binary images: computer algorithms versus mathematical theory. Geoderma **134**(3–4), 284–294 (2006)

Research of the Spindle Units for Multioperational Lathes in the APM WinMachine Environment

Oleg Krol(✉) and Volodymyr Sokolov

Volodymyr Dahl East Ukrainian National University, 59-a, Central Ave., Severodonetsk 93400, Ukraine

Abstract. The problem of modeling the spindle unit's design for multi-operational lathes equipped with a set of modular tooling according to the rigidity criterion is considered. Structural and calculation schemes of a two-support structure in the form of a constant cross-section beam on duplexed angular contact ball bearings considering linear and angular stiffness are proposed. The procedure for constructing an analytical static formula of a spindle as an analytical dependence of its general compliance on the cantilever's dimensions is used, which adequately reflects the conditionally constant (spindle on two supports) and replaceable (modular tooling) parts of the object under consideration. With the help of this formula, it is possible to express procedure probing the machine's working space according to the compliance indicator. Analytical dependencies for finding a rational ratio of the spindle main design parameters from the standpoint of maximum rigidity are proposed. This approach is most effective for typical double-support spindles equipped with a variety of tooling. The efficiency of the APM Structure3D module in solving problems of assessing the stress-strain state, considering the complex mechanism of deformations in supports, is shown. The stress fields, which predetermine the picture of the researched object's deformation state, are presented. For a comprehensive study of the spindle unit, the capabilities of APM Structure3D to determine the set of natural frequencies and the corresponding vibration modes are used.

Keywords: Machine tools · Spindle-cantilever stiffness · Optimal size ratio · Static formular · Stress field

1 Introduction

In connection with the increase in machining processes' productivity and efficiency, the issue of modeling the forming units of metal-cutting machines in modern CAD systems is becoming increasingly important. The analysis of the balance of flexibility and vibration modes of the primary units of lathes showed that the central forming units: spindle – workpiece and support group – tool block, predetermine the quality of the machine as a whole. The spindle's rigidity and vibration resistance characteristics on elastic supports depend on the size of the cantilever part of both the spindle itself and the length of the

V. Ivanov et al. (Eds.): DSMIE 2021, LNME, pp. 41–51, 2021.
https://doi.org/10.1007/978-3-030-77719-7_5

workpiece. Fixing a processing scheme with a particular overhang and building on these basic design schemes and 3D models of the main units of the machine [1, 2] do not make it possible to effectively control the rigidity and vibration resistance within the working space of the machine. In [2], a library of models of generalized multi-axis machine tool configurations is presented.

The widespread introduction of the 3D modeling apparatus in designing machine tools is also presented in [3]. Comprehensive research of the operability of machine tools and technological equipment is carried out using CAD SOLIDWORKS and CAE ANSYS software. Within three-dimensional libraries, 3D models of the spindle and its research by the finite element method are presented. As the author notes, choosing the best modeling method is key to creating an accurate model. The main apparatus of the 3D modeling software is CAD SOLIDWORKS to create the spindle model. To effectively use the finite element method, the CAE ANSYS interface is used for import from SOLIDWORKS, followed by an analysis of the spindle's stress-strain state using ANSYS. Often, spindle researchers use multi-node bar models with three degrees of freedom at each node. For these models, the dynamic characteristics at natural frequencies and modes of vibration of the spindle are carried out, taking into account the changing load. Authors often follow the path of simplifying the original 3D model (removing chamfers and small holes, and other structural elements) when converting 3D file formats between SOLIDWORKS and ANSYS.

An integrated approach to assessing the indicators of rigidity and vibration resistance is presented in [4]. The idea of a modular modeling system based on information about the forming units: spindle-tool and table-workpiece are proposed. The universality of such a structure for presenting information is provided by analytical models and arrays of experimental data, concentrated in the databases' corresponding sections. This article [4] identifies critical parameters and associated constraints based on the data embedded in the database on the characteristics of machine elements' dimensions and rigidity, coordinate matrices, and node vectors. Simultaneously, the issues of the optimal ratio of the spindle size and the tooling component to maximize rigidity and the relationship with the finite element analysis procedure are not addressed in this work.

A promising approach is an approach to constructing the static formula for s_f of the spindle, presented in [5]. This approach is effective when using unified spindle units equipped with a wide range of modular tooling. Simultaneously, the authors considered one variant of loading with a single cantilever force without considering various loading schemes, particularly the forces in the gearing "gearbox output shaft – spindle".

2 Literature Review

The research of the spindle units' structures of metal-cutting machines according to the criterion of rigidity and the influence of technological tooling on design decision-making is widely presented in the machine-tool literature.

In [6], determining the accuracy of the technological operation of boring holes when changing the dimensional parameters of the spindle unit (SpU) and its rigidity is considered. When obtaining an analytical expression for the SpU compliance, considering the spindle's deflection and its supports, the value of the restraint force in the front support was taken into account. The advantage of this work is to consider the variety of boring machine tool designs. Simultaneously, as is known, the parameters of their matching (joint) also affect the level of deformations of the "boring bar – boring cutter" assembly, which in turn affects the rigidity of the forming spindle unit. It is an aspect of the influence of tooling that is not considered in this work. Information about the features of the influence of duplexed angular contact ball bearings and, in particular, the consideration of their angular compliance on the stiffness of the SpU as a whole is also not given.

The work [7] considers the nature of the relationship between the stiffness characteristics of the forming units of multi-operational machines of the drilling-milling-boring type for processing accuracy. Of interest is a new approach associated with the study of the space of change in static stiffness by introducing the concept of "generalized stiffness", covering the machine tool's entire working area. The authors implement the procedure for forming 3D and parametric models on the scale of multi-axis processing space. This achieves an effective procedure for assessing and predicting possible processing errors. Nevertheless, at the same time, the procedure for changing the technological tool is not presented in work. The task of finding the ratio of the dimensions for the inter-support part of the spindle and the cantilever part, reflecting the dimensions of the technological tooling, providing minimal deformations of the forming unit, is not posed either. The same approach to assessing stiffness is used in [8] but without advanced 3D modeling and parameterization tools.

The great opportunities in terms of automation of the main procedures for evaluating structures by the stiffness criterion are provided by the integrated CAD APM WinMachine [9, 10], which includes the APM Structure3D module – a module for calculating the stress-strain state, stability, natural and forced vibrations of parts and structures by the finite element method [11]. In this system, a more efficient procedure is proposed for determining the stiffness of structural supports considering linear and angular compliance.

Based on the analysis carried out, the task of this study can be formulated as follows: To develop an analytical toolkit for assessing the stiffness of a double-bearing spindle assembly and the choice of the optimal ratio of the sizes of its elements using various types of technological equipment in the environment of the APM Structure-3D module.

3 Research Methodology

3.1 Determination of the Spindle-Tooling Structure Stiffness

Consider a variant of combined loading of a unified two-bearing spindle unit (Fig. 1) for a multi-purpose lathe mounted on duplexed angular contact ball bearings 4-46209 and 4-46112, mounted according to the "tandem-O" scheme with a spring-type preload (rear support) and a preload using two spacers for duplexed front support [12, 13].

Let us consider the problem of calculating the rigidity of the spindle unit's structure (spindle-modular tooling) of the main motion drive for a multi-operational lathe (for example, model MS03), the structural diagram of which is shown in Fig. 1b.

This spindle unit design can be presented in the form of a constant cross-section beam on two hinged supports, the design diagram of which is shown in Fig. 1c.

At the same time, the rolling bearings on the rear (r) and front (f) bearings have finite stiffness, and their action in the design scheme can be conditionally replaced by springs with stiffness j_r and j_f (the springs can perceive both compressive and tensile stresses). This assumption is in good agreement with practice if the bearings are preloaded. The rigidity of bearings 4-46112 GOST 831-75 (front support) and 4-46209L GOST 831-75 (rear support) can be determined analytically or graphically. Using the graph [1], we determine the rigidity of the above duplexed angular contact bearings: $j_r = 8.8 \cdot 10^4$ N/mm – for bearings 4-46209L; $j_f = 9.2 \cdot 10^4$ N/mm – for bearings 4-46112.

The radial compliance A of the rear and front supports will be $A_r = 0.113\ 10^{-4}$ mm/N and $A_f = 0.109\ 10^{-4}$ mm/N, respectively. The radial compliance of support consisting of several angular contact ball bearings is determined by the formula [1] and is $0.652 \cdot 10^{-5}$ mm/N. The presence of a preload $P_{pl} = 930$ N in the front support, following the recommendations [1], increases the rigidity by 15–20%; in this case, the front support Af's compliance $0.522 \cdot 10^{-5}$ mm/N.

To determine the analytical model for assessing the spindle unit's compliance with the MS03 machine tool, we will use the method of initial parameters in the matrix formulation [5, 14]. According to the proposed design scheme, the SpU is represented as a statically indeterminate elastic system "spindle-cantilever" (S-C) on two supports that have linear $\{A_r; A_f\}$ and angular $\{a_r; a_f\}$ by compliances with 4 unknowns: reactions in the rear and front support $\{R_r R_f\}$ and corresponding reaction moments $\{m_r m_f\}$ in these supports.

To assess the characteristics of the spindle unit's compliance considering the size of the machine working area, the program was developed in the mathematical environment "Maple". Using the kernel of symbolic mathematics, a static form was obtained $s_f = f(l_k)$ for various cantilever lengths l_k of the spindle unit (e.g., multi-operational machine MS03).

We represent the mathematical model of the S-C system in the form of a matrix Eq. (1):

$$\begin{bmatrix} 1 & 1 & 0 & 0 \\ l + l_1 & l_1 & -1 & -1 \\ A_r - \frac{l^3}{6EI} & -A_f & a_r l + \frac{l^2}{2EI} & 0 \\ \frac{-l^2}{2EI} & 0 & a_r + \frac{l}{EI} & -a_f \end{bmatrix} \times \begin{bmatrix} R_r \\ R_f \\ m_r \\ m_f \end{bmatrix} = \begin{bmatrix} R' \\ -R' l_k \\ 0 \\ 0 \end{bmatrix}, \tag{1}$$

where l – inter-support distance, mm; l_1 – length of the cantilever part of the spindle, mm; l_k – length of the cantilever (modular equipment and workpiece), mm; E – elastic modulus of structural steel – Steel 20X, $E = 2.1 \cdot 10^5$, MPa; I – a moment of inertia of the spindle cross-section, mm^4; R' – the unit force applied at the cutting point, N.

With the help of the above-developed program in the Maple environment, a static formula for s_f of the SpU machine model MS03 was obtained, presented in the form of an analytical dependence of the spindle compliance (taking into account the support compliance) on the length of the cantilever:

$$s_f = 0.29 \cdot 10^{-4} + 0.332 \cdot 10^{-6} l_k + 0.507 \cdot 10^{-8} l_k^2. \tag{2}$$

The resulting analytical formula is an effective toolkit for determining and modeling the characteristics of rigidity within the machine's working space. A similar approach for

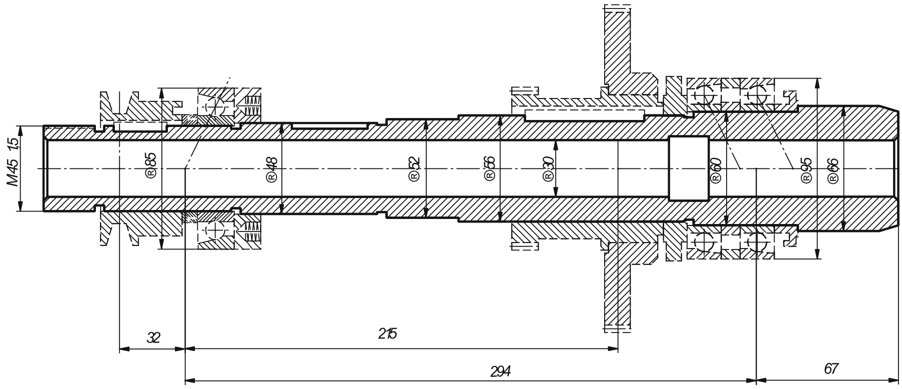

a

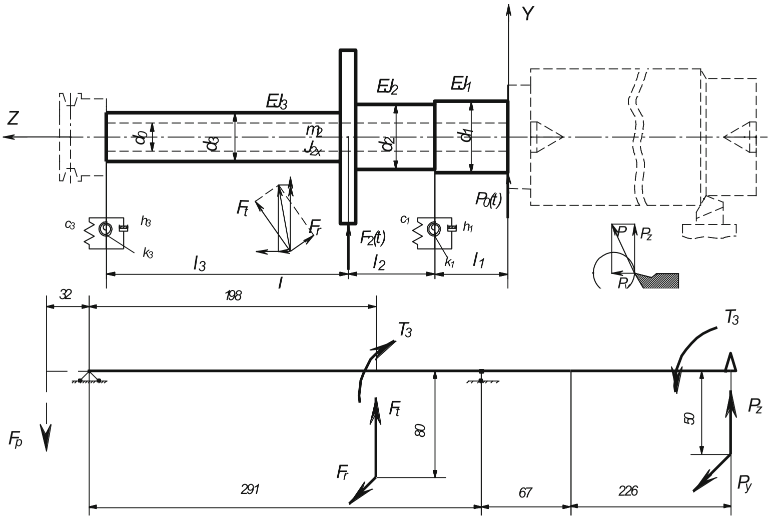

b

Fig. 1. Spindle unit: a – spindle design; b – structural diagram of the spindle with tooling.

the problem of optimizing the design of a fixture for multi-axis processing of lever-type parts with statistical and modal analysis is presented [15]. The resulting static formula for s_f becomes promising in the problem-oriented analysis of complex details [16, 17].

3.2 Finding the Optimal Ratio of Spindle and Cantilever Sizes

A specific reserve of the spindle structure's rigidity can be formed depending on the ratio of its main parameters: the inter-support (spindle span) distance l and the span diameter d_0 [18, 19].